

THE PENNSYLVANIA STATE UNIVERSITY
SCHREYER HONORS COLLEGE

DEPARTMENT OF BIOENGINEERING

**FEASIBILITY STUDIES FOR OPTICAL TRAP DETECTION OF SINGLE MOLECULE
ADHESION AND FORCE GENERATION**

DAVID J. BERNICK
Spring 2012

A thesis
submitted in partial fulfillment
of the requirements
for a baccalaureate degree
in Bioengineering
with honors in Bioengineering

Reviewed and approved* by the following:

Peter J. Butler, Ph.D.
Associate Professor of Bioengineering
Honors Advisor
Thesis Supervisor

William Hancock, Ph.D.
Associate Professor of Bioengineering
Faculty Reader

Keefe Manning, Ph.D.
Associate Professor of Bioengineering
Faculty Reader

* Signatures are on file in the Schreyer Honors College.

ABSTRACT

The optical trap (laser tweezers) is an instrument which uses laser radiation and the focusing power of a microscope to trap microscopic particles such as beads, bacteria, and organelles. The particles are pulled into the focal point of the trap and held in three dimensions by the transfer of the photons' momentum. The resultant force (F) can be modeled as a Hookean spring, $F = k_{spring} x$ with the forces used to hold the particle dependent on the particle's displacement (x) from the trap center. Optical traps and can measure forces at the piconewton level.

It has been reported that during binding reactions between receptors and ligands, piconewton forces and nanometer displacements are produced on time scales that are on the order of micro- to milliseconds. Thus, an optical trap is an ideal instrument to detect these events as they happen, provided the position detection can be accomplished at these very short time scales.

Previously, our optical trap measured displacements using a CCD camera followed by displacement assessment using image correlation-based tracking. This method had a disadvantage in that it could only measure positions up to about 50 Hz and required simultaneous differential interference contrast imaging of the bead. The requirement for imaging can be a disadvantage when it is desired to use the microscope to detect other events based on fluorescence. The focus of this study was to integrate a Quadrant Photodiode (QPD) into a conjugate focal plane behind the condenser. A QPD, when properly aligned and calibrated, can detect the changes in laser beam position caused by small movement of the bead in the trap. The update rate of the QPD is about 30 kHz allowing three dimensional tracking of bead position of greater than 10 kHz using an analog to digital converter.

Thus the main aims of this research were to (i) determine the range, measured from the coverslip surface, within which the k_{spring} is constant, (ii) determine the relationship between QPD voltage and bead displacement from the trap center, (iii) assess the feasibility of measuring rapid binding events, and (iv) conduct preliminary studies on the detection of binding events between a fibronectin functionalized bead and integrin receptors on the endothelial cell surface.

TABLE OF CONTENTS

LIST OF FIGURES	iv
LIST OF TABLES	vi
ACKNOWLEDGEMENTS	vii
Chapter 1 Introduction	1
Optical Trap	1
Binding Forces	2
Chapter 2 Instrumentation	5
Optical Trap	5
Setting up the Microscope	7
Microscope Stage	7
Culture Dish	8
Condenser Set Up	8
Differential Interference Contrast Set Up	9
Laser	10
Laser Path	11
Lenses Used	12
Image Tracking	12
CCD Camera	14
Image Position Detector	14
LabVIEW Programs	15
Chapter 3 Methods	20
Spring Constant	20
Attaching Beads to the Cover Slip	20
Calibration of the Quadrant Photodiode	22
Detection of Single Binding Events	24
Bead Binding to Cells	25
Chapter 4 Results & Discussion	27
Beads at Different Distances from Surface of Cover Slip	27
Calibration of the Quadrant Photodiode	29
Detection of Single Molecule Binding Events	38
Bead Reactions with Bovine Aortic Endothelial Cells	42
Chapter 5 Conclusion	46
Conclusion	46
References	47

Appendix A Raw Data Images	50
Appendix B Readme Instruction File: Directions for Particle Tracking	52
Appendix C Academic Vita	54

LIST OF FIGURES

Figure 2-1: A digital image of the optical trap	6
Figure 2-2: A typical culture dish	8
Figure 2-3: DIC schematic	9
Figure 2-4: Laser Path schematic	11
Figure 2-5: Imaging cross-correlation schematic	13
Figure 2-6: Tracking images using LabVIEW software, “Multiple Particle Tracking.vi”	16
Figure 2-7: Tracking QPD voltages using “q4d readout w trigger.vi”	18
Figure 2-8: Tracking QPD voltages using “Step displacement of nanostage with high rate QPD”	19
Figure 3-1: Image of avidin and biotin binding	21
Figure 3-2: Laser on QPD.	24
Figure 3-3: Bead coated with avidin, surface coated with biotinylated fibrinogen	25
Figure 4-1: Calibration of optical trap at different distances from surface	27
Figure 4-2: Spring stiffness and QPD variance vs. bead height	29
Figure 4-3: Bead moving in X direction	30
Figure 4-4: Tracking of imaged bead in X direction using tracking LabVIEW program	32
Figure 4-5: Tracking of imaged bead in X direction using QPD and stage sensor	33
Figure 4-6: Graph of x axis average QPD readout (μm) versus tracking software position (μm).	34
Figure 4-7: Graph of x-axis calibration for QPD	36
Figure 4-8: Graph of y-axis calibration for QPD	38
Figure 4-9: Bead coming close to bFN surface using optical trap	39
Figure 4-10: Raw QPD data, displaying rapid adhesion to FN surface	41
Figure 4-11: Fibronectin coated 2 μm bead held in place on the bovine nerve cell surface using optical trap	43

Figure **4-12**: Raw QPD data, displaying focal adhesion of a fibronectin coated bead to the bovine nerve cell extracellular proteins.

44

LIST OF TABLES

Table 2-1: Lenses used in laser path	12
Table 3-1: Equations for QPD voltage readout	23

ACKNOWLEDGEMENTS

I would like to give a big thank you to Dr. Peter Butler for all the time, effort, and understanding he has shown me both in the lab and during this writing process. I now have an understanding and an appreciation of what research is and how difficult it is sometime to achieve a result. I would also like to thank the faculty readers, Dr. Keefe Manning and Dr. William Hancock for reviewing this thesis; I hope it reminds you of your first experience in research.

“Writing is never finished. It's just due.” ~ Kelly Gallagher

Chapter 1

Introduction

Optical Trap

The optical trap is an instrument composed of a microscope and a laser beam which uses the laser radiation to trap microscopic particles. Using the focusing capabilities of the microscope, the laser light is brought to a single point where the momentum transfer of the photons can produce piconewton-sized forces, trapping microscopic particles in three dimensions. The size of these particles range from 0.1 microns to 100 microns, such as beads (Stout, 2001; Jeney, 2010), chromosomes (Vorobjev, 1993), human gametes (Conia, 1994), micronuclei (Aufderheide 1993), kinesins (Kuo, 1993; Stelzer 2004), and myosin (Molloy,1995).

An optical trap is formed by tightly focusing a laser beam with an objective lens of high numerical aperture (NA) (Neuman et al., 2004). This arrangement permits a beam with Gaussian distribution of intensity to enter the focal volume at a steep angle. The steep intensity distribution along with the steep angle of light propagation results in a high trapping force. The maximum numerical aperture is based on the index of refraction of the medium immediately following the objective. In our setup we use an oil immersion objective with a numerical aperture of 1.45, (Williams, 2001). Particles near the beam's focus experience forces from the refraction of light from the scattering of incident photons, and the laser light gradient. The first is from the scattering of light and the absorption of photons which transfers momentum and pushes the bead in the direction of the light rays. The gradient force is more important to trapping and results from the intensity gradient near the focus of the laser. In order to trap in three dimensions, the axial force of the gradient force at the focal point must be greater than the scattering force pushing it away. This is achieved by focusing a Gaussian laser beam using a high NA objective, creating a steep cone-shaped gradient of light (Neuman et al., 2004).

The theory behind this optical force based on simple ray optics. When incident photons go through a bead, they are refracted due to a change in refractive index of the medium. This causes a change in direction of the beam of light which corresponds to a change in velocity of the light. A change in velocity means a change in

momentum (p) carried by the photons, $dp/dt = m \cdot dV/dt$. By the law of conservation of momentum, this causes an equal and opposite momentum change in the bead, $dp_{\text{photon}}/dt = dp_{\text{bead}}/dt$. The rate of this momentum change acts as a force on the bead, which is proportional to the light intensity or number of photons present, $dp_{\text{photon}}/dt = F_{\text{bead}}$. Therefore, using a Gaussian laser light, with the greatest intensity of light at the central axis and dissipating toward the edges, the bead is drawn towards the center of the laser light, and is effectively “trapped” there.

For small displacements the gradient force is proportional to the displacement from the equilibrium position, and in practice the trap can be modeled as a weak Hookean spring whose stiffness is proportional to the light intensity and distance of the bead from the trap center. These features can be used to find a spring constant k_{spring} , determined by equating the variance of displacement with the thermal fluctuations according to the equipartition theorem; $U = \frac{1}{2} k_{\text{spring}} x^2 = \frac{1}{2} k_{\text{boltz}} T$, where U is the potential energy, k_{spring} is the spring constant, k_{boltz} is the Boltzmann constant, and T is the temperature at which the experiment occurred. Alternatively, the trap strength can be measured by finding the displacement x of the bead due to known applied force, F , e.g., from fluid flow: $F = k_{\text{spring}} x$.

Binding Forces

Besides manipulating microscopic particles, an optical trap is also suitable for measuring the biological force of molecular interactions. Once trapped, a bead can be steered into position in order to bind with a partner molecule attached to a cover slip. To bring about ligand–receptor interactions and focal adhesions, receptors and their ligands must be anchored onto two opposed surfaces, called two-dimensional interaction. Regulation of cell adhesions is based on the kinetic rates and governing factors of ligand–receptor interactions (Sun et al. 2009). Dissociation kinetics (Sun et al. 2009), and forced bond rupture (Stout, 2001; Jeney, 2010) have been investigated experimentally using the optical trap.

Sun et al. investigated the kinetics of receptor–ligand interactions governing cell adhesion using an optical trap-based thermal fluctuation approach, to visualize two dimensional kinetic bond formations (Sun et al. 2009). The kinetics of carrier diffusivity were assessed when thermal fluctuation-assisted adhesion (thermal fluctuations measurement) and with trap-assisted adhesion (adhesion frequency measurement). The thermal

fluctuation measurement was found to reduce the contact time of the two surfaces. In adhesion frequency measurements, however, two surfaces were forced into physical contact for the entire contact duration, increasing the kinetic rate. An increase in the trap stiffness also increases the kinetic rate. This change in kinetic rates can be used in experiments for single molecule events. By using thermal fluctuation and decreasing the kinetic rate, the likelihood of a single binding event can be increased.

Stout et al. characterized single molecule force measurements of intermolecular bonds using an optical trap (Stout, 2001). Using a piezoelectric stage moving at a set rate in the X and Y planes, ligand-coated beads were trapped a short distance from a receptor-coated cover slip. When the bead managed to bind to a surface-bound receptor, it is pulled away from the equilibrium position with the velocity of the moving stage. Eventually, the total force applied to the bead by the trap and the surface overcame the adhesion due to the receptor-ligand interaction. The bond broke, and the bead returned to the trap. These results were designed to detect individual protein-protein interactions and measure the forces required to rupture them. (Stout, 2001)

Jeney et al. introduced a similar method for single molecule force measurements of ligand–receptor interactions using the photonic force microscope, of similar concept to the optical trap system. Unique to this approach was that the piezoelectric stage moved only in the Z direction. Biotin-coated beads were steered towards a streptavidin coated cover slip; bound, pulled, and unbound, to measure the effect of different pulling forces on the lifetimes of individual streptavidin–biotin complexes. (Jeney, 2010)

Chen et al. used an antibody-coated bead in an optical trap to observe the manipulation of single receptors on the extracellular membrane of natural killer cells (Chen, 2007). Using known values after calibrating the spring stiffness of the trap, adhesion forces between a bead and a cell for each binding event were calculated from the maximum displacement of the bead from the trap center. Results demonstrated that the adhesion forces between the antibody and the bead were time-dependent.

This thesis explains the way an optical trap works, along with the methods of setting up and calibrating the instrument. Similar experiments will be conducted in which avidin-coated beads are trapped and brought close to biotinylated fibronectin adsorbed onto a coverslip. In addition, pilot experiments are described in which a bead with fibronectin is trapped and brought close to a cell in order to induce focal adhesion formation.

The main aims of this research are to (i) determine the range, measured from the coverslip surface, within which the k_{spring} is constant, (ii) determine the relationship between QPD voltage and bead displacement from the trap center, (iii) assess the feasibility of measuring rapid binding events, and (iv) conduct preliminary studies on the detection of binding events between a fibronectin-functionalized bead and integrin receptors on the endothelial cell surface.

Chapter 2

Instrumentation

Overview

In this chapter, the main components of the optical trap are introduced including the objective, stage, condenser, laser, CCD camera, and quadra photodiode. Also provided are details of the protocols users should follow when setting up the optical system for trapping beads.

Optical Trap

The main components of the optical trap in use in the Mechanotransduction Laboratory are a fiber coupled laser diode and an inverted microscope (Olympus IX71). The microscope is combined with a CCD camera to record microscope images, shown in Figure 2-4.

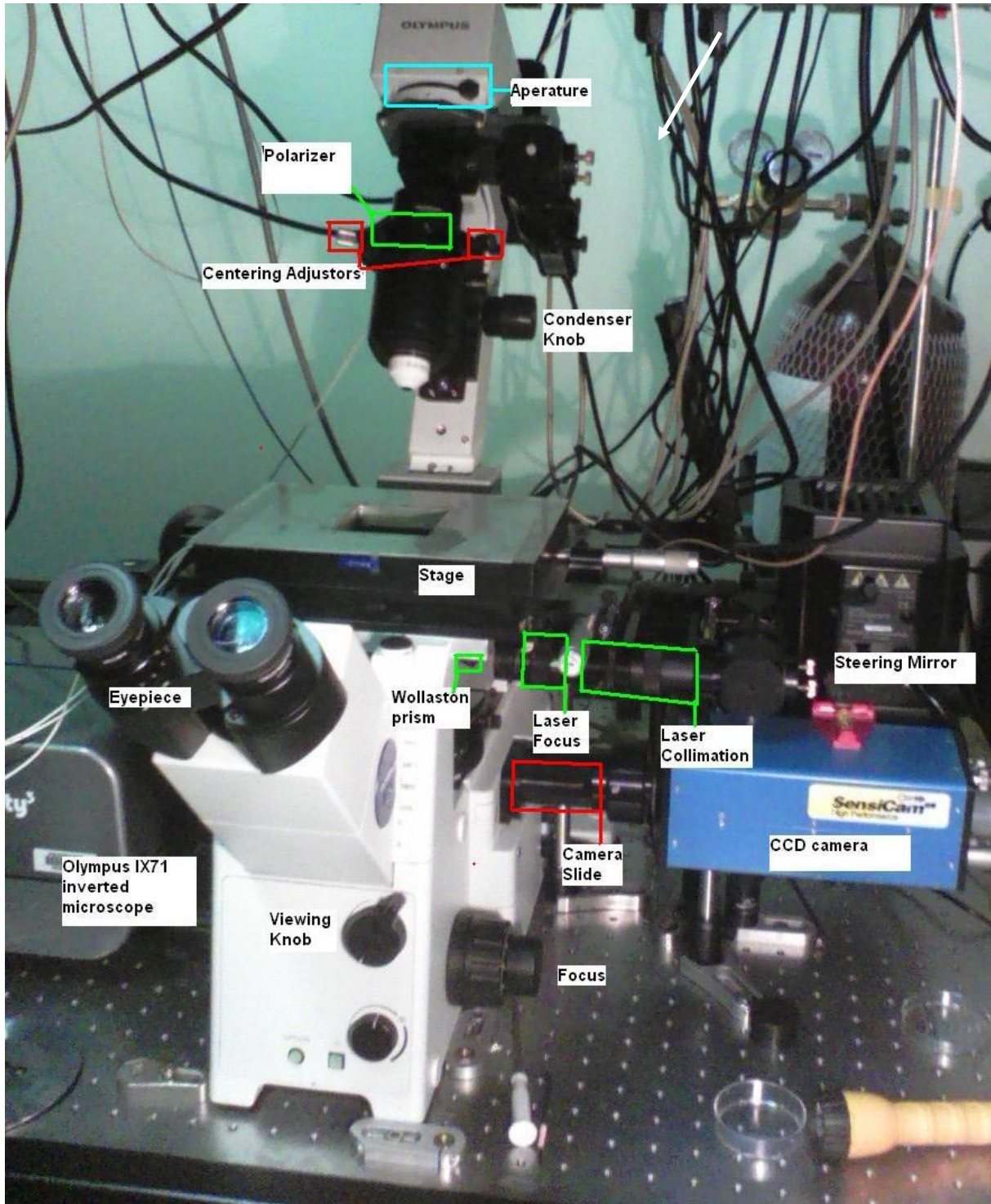


Figure 2-1: A digital image of the optical trap, courtesy of The Pennsylvania State University's Bioengineering Department. The labeled parts of the microscope are used to set up the optical system for trapping beads.

Setting up the Microscope

The microscope in use is an Olympus model IX71 inverted confocal light microscope. Before using a microscope for any application, the stage and condenser must be set up according to the application. This series of instructions is for setting up an inverted microscope for optical trapping using differential interference microscopy (DIC) to view the samples.

To begin setting up the microscope, the correct objective must be used. For optical trapping applications a Plan Apo N oil objective is used (60x/ 1.45 Oil, ∞ /0.13-0.19/FN26.5, from Olympus). This is a normal field of view apochromatic and flat field correction type objective. The objective provides 60 times magnification with a numerical aperture (NA) of 1.45 when used with oil with a refractive index of 1.515. It is infinity corrected with the cover glass thickness range of 0.13 – 0.19 and a Field Number (FN) or Field of View of 26.5. When using an objective with a high NA it is important to set the correction collar of the objective to the coverslip glass thickness in mm, the standard coverslip glass has a thickness of 0.17 mm, so the normal is 0.17. Cover glass thicknesses can vary and even variation of a few tenths of millimeters can result in image degradation due to aberrations (Davidson, 2009). To insert the objective, the objective cover on the microscope, located directly beneath the stage is unscrewed and replaced with the Plan Apo N oil objective. Next, 15 μ L of 1.515 oil is pipetted onto the top of the objective lens. It is important that not so much oil is used since it can drip off the lens. This oil can get inside the objective and inhibit its functionality, which would require the objective to be sent back to the company for cleaning.

Microscope Stage

The microscope stage is movable with piezoelectric motors, powered by a Nano-Drive by Mad City Labs, Inc. and is controlled by the LabVIEW program “Step displacement of nanostage.vi” and “Step displacement of nanostage with high rate QPD.vi”. This stage has the capability of moving in 1 nm increments with 0.1nm of precision in the positive and negative x, y, and z directions, with up to 100 μ m of displacement in each direction.

The stage must be set for the culture dish to be used. This can be as simple as setting a stage cover (circular disc with a hole in the center) on the stage, or using a stage adapter which connects directly to the stage and can hold culture dishes and control temperature for cellular applications. It is important to have enough room above the stage so that the objective can be raised and lowered for focus without touching the glass bottom of the culture dish.

Culture Dish

At this point the culture dish may be placed on the stage. This dish is used to contain the samples while trapping occurs. The objective should be raised just enough so the oil on the objective lens touches the cover slip, but not so much that the lens touches the glass bottom of the culture dish. A sample of 1000 μL of water (or PBS depending on the application) should be pipetted into the culture dish along with a sample beads, typically 1-4 μL depending on concentration and size of the beads.



Figure 2-2: A typical culture dish used to contain samples; the sides of the dish are sloped to contain the liquid sample. (Delta T Dish Black courtesy of bioprotechs.com)

Condenser Setup

The condenser is at the top of the microscope and should be tilted back when not in use for easy cleaning and access to the stage. First bring the condenser forward so that it is positioned above the culture dish. Using the condenser knob – located at the back – dip the tip of the condenser lens into the sample water in the culture dish. The water should adhere to the lens and form a sort of curve. To view the sample through the microscope, turn the condenser light on, turn the viewing knob to the viewing setting – it looks like an eye – and push the slide connecting the camera to the microscope towards the microscope. Close the aperture at the top of the condenser all the way, this is so that the condenser light may be positioned.

This next step can be the most difficult and time should be taken so that it is done correctly. The focal plane of the microscope must first coincide with the position of an object near the normal trapping location. In order to accomplish this, first focus on something near the coverslip. Ideally the top of the coverslip should be found, but a sample or bead can also work. Slowly bring the objective up to the coverslip by turning the top of focus knob towards you while observing through the eyepiece. Care should be taken that the objective does not bump into the coverslip. It is important to focus on the top of the cover slip and not the bottom, this can be done by first finding a sample (floating bead) and bringing the objective up to the surface of the cover slip. A good way to find the surface is to look for anything that may be attached and sitting on the cover slip such as dust particles, proteins, or beads.

The next step is to close the condenser aperture iris and move the condenser knob to focus the condenser. When the condenser is in focus, the light will appear bright surrounded by a dark octagon. Focus the condenser so that the edges of the octagon are clearly in focus. A red or blue halo around the octagon may be seen, but this is an aberration and not a problem. Use the condenser centering adjustors (two knobs on either side of the condenser tube) to move the octagon of light to the center of the viewing area. Open up the aperture so that all of the points of the octagon touch all of the edges of the viewing area, ensuring the condenser light is centered correctly. Finally, open up the aperture just enough that the octagon can no longer be seen, but do not open the aperture all of the way. Enough light should be in the viewing area but not so much to overexpose the area.

Differential Interference Contrast Setup

Differential interface contrast microscopy (DIC) is a method of viewing transparent specimens by

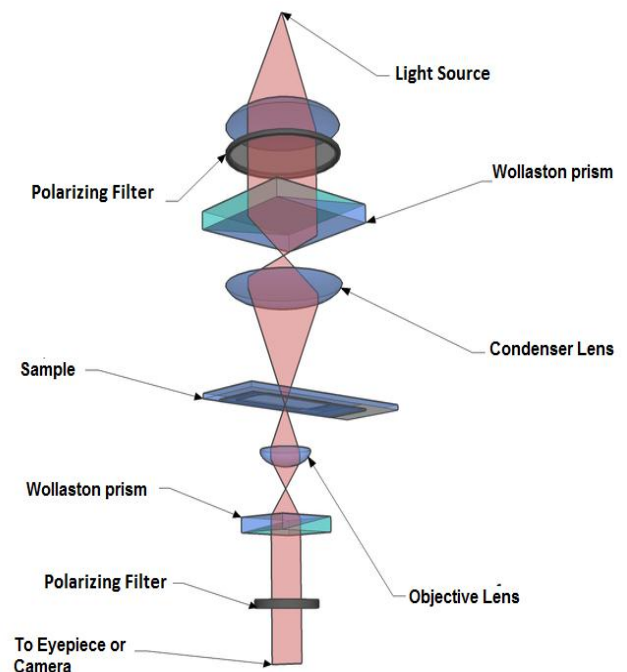


Figure 2-3: DIC schematic used in an inverted microscope.

generating contrast that depends both on sample refractive index and sample thickness. Figure 2-2. To achieve a good DIC image, first pull out the bottom Wollaston prism (black on the right side corner), and remove the right eyepiece of the microscope. Look down the eyepiece. A bright light with a dark line through the center should be visible, called the Becke Line. If not visible, rotate the top polarizer (a wheel on the condenser tube) until the line is as dark as possible. Replace the bottom Wollaston prism and eyepiece and view the sample, adjusting the bottom prism knob as necessary until the sample achieves a dark and light pattern. On a bead, there should be a crescent of light on one side with shading to dark, see Figure 4-9 for a good example. The background view should have a slight gradient of light to dark.

Now the microscope is all set up and ready to view samples. It should be noted that the microscope viewing should be switched to the CCD camera *before* the laser is tuned on to prevent any laser light from entering the eyes. This can be achieved by turning the viewing knob to the camera setting – it looks like a camera – and pushing the slide that operates a mirror, directing light to the camera.

Laser

The most basic requirements for a laser suitable for trapping is one with a Gaussian mode output with pointing stability and low power fluctuations (Neuman, et al., 2004). This will allow for a small diameter beam waist and therefore an efficient, harmonic trap. Pointing instabilities would lead to displacements of the focal point and therefore decreased trap stiffness. Any fluctuations in power would lead to variations in the trap stiffness.

The output of the laser determines the stiffness of the trap and therefore the maximum possible force. As a rule of thumb, the maximum trapping force that can be achieved with micron scale beads is on the order of 1 pN per 10 mW of power (Neuman, et al., 2004). Therefore it can be estimated that our current laser, operating at 50 mW could provide a trapping force of 5 pN.

The wavelength of the laser is important to consider when trapping biological material such as cells or small organisms. There is an ideal portion of transparency in the infrared spectrum (~750–1200 nm), which

allows a high enough wavelength to prevent the absorption of proteins in the visible, while a low enough wavelength to limit the increasing absorption of water in the infrared. There is still optical damage which can occur to biological specimens in this infrared range, with damage minima occurring at 970 and 830 nm. The laser used in the current optical trap has a wavelength of 830 nm, making it ideal for trapping biological specimens.

Laser Path

The laser light is emitted from the iFLEX-1000 (Qioptiq, formerly Pointe Source), a fiber-coupled laser diode system with a fiber output power of 50 mW and an operating wavelength of 830 nm. The light goes through a fiber optic cable, and comes out a collimated diode at about 1 mm in diameter. The light travels to two positioning mirrors which allow the laser to move in the x and y axis of the stage. The laser then goes through a compact beam expander consisting of two lenses, a fine tuner and a shutter. The lenses expand and collimate the beam from 1 mm to ~8 mm in diameter. The fine tuner manually adjusts the length of beam expander. By moving the fine tuner, the collimation can be adjusted which moves the focal point of the trap, ensuring the trapped particle is in the microscope's plane of view. The shutter allows the trap to be "turned off" without unplugging or switching off the laser, providing an easy way of removing particles from the trap. The laser light then enters the microscope and is reflected off of a dichroic filter, which only reflects infrared (830 nm) light, while passing all other visible wavelengths.

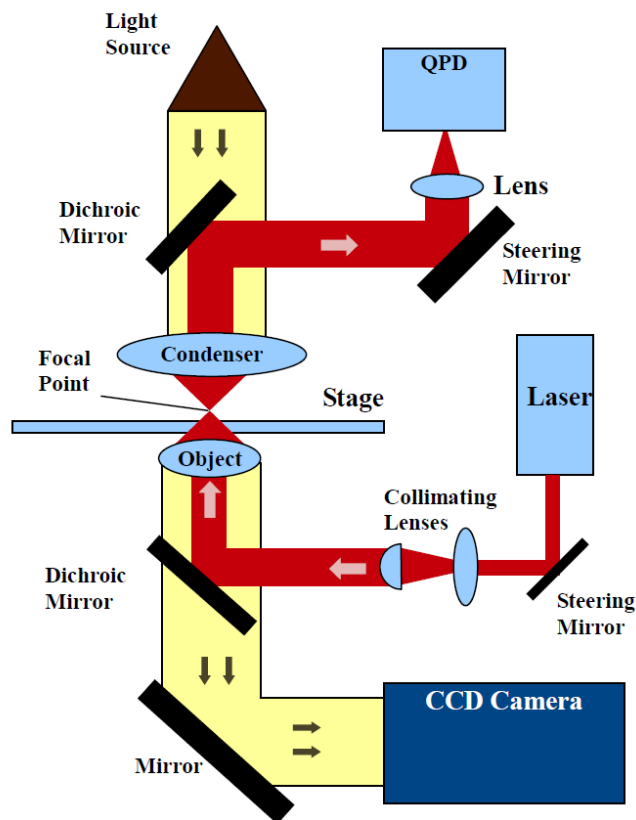


Figure 2-4: Laser Path schematic used for the optical trap, note how the laser light and the condenser light source travel in opposite directions. The focal point is where the trapping occurs.

The reflected light enters the oil immersion objective lens (NA of 1.45), the oil, and into the culture dish which sits just above the objective connected by the oil. The laser continues through the water and into the condenser, which is dipped into the water. The light travels through the condenser and is reflected off of another dichroic mirror, sending the laser beam in a different direction but allows the microscope's light to pass through to illuminate the sample on the stage. The reflected laser beam is sent to another positioning mirror, through a lens into the quadrant photodiode (QPD). The lens narrows the beam to a single point on the QPD.

Lenses Used

Component	Description
Collimation beam	lens 1: 10mm diameter; 10mm focal length; 5mm center thickness
	lens 2: 18mm diameter; 40mm focal length; 7mm center thickness
Objective	Plan Apo N 60x 1.45 Oil
Condenser	IX2-TLW 0.2-0.9
Steering Mirror	2 axis Steering mirror with three knobs
Dichroic Mirror	Passes wavelengths below 730nm, reflects those above

Table 2-1: Lenses used in laser path, two lenses are used in the collimation beam, one for expanding the beam and the other for collimation.

Image Tracking

In order to determine spring stiffness and bead displacement, a method of tracking the particles to within a few nanometers is needed. Recently, Cheezum et al. evaluated specific implementations of four commonly used tracking algorithms: cross-correlation, sum-absolute difference, centroid, and direct Gaussian fit (Cheezum,

2004). This was done by using a range of computer generated (CG) particles, from a point source to 5 microns, with known movements. To make these CG particles realistic, varying amounts of noise were added to simulate various signal to noise ratios. It is found that for the applications of trapping micron sized beads, the cross correlation method is the most accurate tracking algorithm.

In order to implement cross correlation based tracking, we use the method of Gelles, et al. to obtain precise positional information from light-microscope images of bead movements *in vitro* with a precision of 1-2 nm (Gelles, 1998). The key point about this technique is that the method uses positional information from the entire bead image rather than a point or edge, which maximizes the precision of measurement.

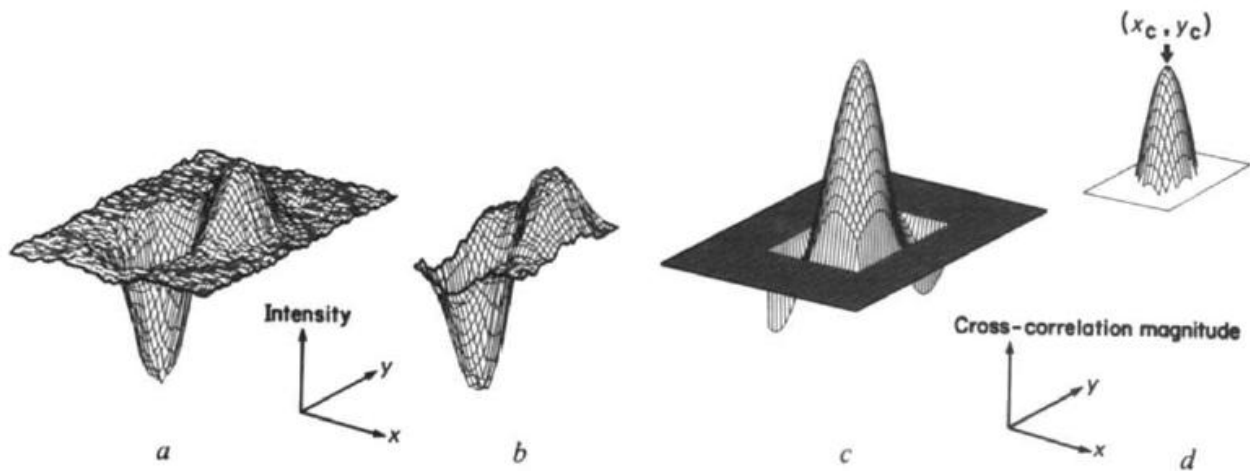


Figure 2-5: Imaging cross-correlation schematic. The first frame of a DIC microscope image of a bead (a) is analyzed for the bead's opposing light and dark areas, and a 'kernel' (b) consisting of the intensities of the bead image is taken. The kernel is used as a template and all of the subsequent images intensity distributions are compared as to how closely they match the kernel's center. The cross correlation (c) of image a with kernel b shows where the intensity distribution in the frame closely matches with the kernel. The peaked region is where the images most closely match each other. Image (d) is a representation of the centroid (x_c, y_c) of the peak is computed and is taken as the position of the bead in a. A sequence of images can accurately show displacements of the bead so long as the image does not significantly change in both intensity and shape. A LabVIEW program based on this technique is used to determine bead displacement and spring stiffness for the optical trap. (image from Gelles, et al., 1998).

CCD Camera

The image from the stage is expanded in the objective, reflects off of the dichroic mirror and through a green wavelength filter to remove the laser light from the image. The image is reflected off of a stationary mirror and into a CCD camera, Figure 2-4.

The camera in use is the SensiCam QE High Performance by Cooke, connected to a computer and is run through the program CamWare. Use the “B+W” (black and white) setting to view the specimen and the “Camera Control” to change the camera settings. Typically images are viewed under “Long Exposure” with a 0 s delay time and a exposure time of 17-26 ms. It is important to set the number of frames to record, as this determines how long the camera records.

In order to view just the laser - typically used to find the trap position - set the “Camera Control” to “Fast Shutter” with an exposure time of 25 μ s and the filter wheel to the FITC cube. To ensure the laser is in the best position, set the microscope focal plane to the top of the coverslip. Using the laser focus, move the beam so that it moves from a series of diffraction patterns, until it appears as a small dot. The laser can be moved in the X and Y axis using the steering mirror knobs to find the position where the laser is most like a circle. Upon trapping a sample, the laser focus may be re-adjusted so that the sample is in the focal plane.

Imaging Position Detector

An alternative method to visual tracking is to image the laser onto a quadrant photodiode (QPD), which allows for high-bandwidth detection. The QPD is a 2 x 2 array of individual photodiode active areas, separated by a small gap, fabricated on a single chip. This maximizes the uniformity and performance matching between the four individual elements. When the laser light hits the active photodiode, it reacts and a voltage is produced. If the QPD is integrated into the trap, downstream of the trapped particle, we can determine the bead's movement; when the bead moves away from the center of the trap, even slightly, the laser beam also moves. We can measure how far the laser is from the center of the QPD by the voltage produced. Unlike CCD imaging which can take images

of the bead's movement from 20 to 60 frames per second, the QPD can measure up to 30 kHz . Since certain proteins can bind to each other with time scales on the order of 1 to 1/10,000 seconds, this system should be able to measure individual molecular binding events.

LabVIEW Programs

Several programs were used to image the beads and track the beads using images and the QPD. To track the beads visually, the program CamWare was used to capture images from the camera. A region of interest was specified around the trapped bead and images were taken as 16 bit .tiff files. These files were opened using the program ImageJ, which converted the file into 8 bit format and then each frame was saved as an individual image using a Save As => Individual Stacks command. This procedure saved each frame as a separate image in sequence. A custom LabVIEW program written by Jhanvi Dangaria, called "Multiple Particle Tracking.vi", was used to analyze and track the movement of the bead in each frame using a cross correlation technique (Gelles, 1998), see Figure 2-6.

To use the LabVIEW "Multiple Particle Tracking.vi", run the VI and enter the Frame Rate and Tracking Time. The frame rate can be found on the "Camera Control" window at the bottom by pressing the "Info" button. The tracking time is the number of frames recorded divided by the frame rate. The user should make sure to round down this value before entering the value into the tracking VI. (See Appendix C Readme Instruction File).

Next, click the button "Load Image", to load the first frame of the image stacks. This will open up a new window labeled "Select a Rectangle". Select the area around the bead to be used as the region of interest (the zoom tool is helpful here) and click "OK". It is important to select a region slightly larger than the sample about 2 - 3 pixels beyond the sample, but not so large that the selection rectangle touches the edge of the image. For the typical 1 μ m bead, an area of 22 x 22 pixels was selected. A larger region of interest will not significantly change the particle tracking data. Another "Select a Rectangle" window appears if a second particle needs to be tracked. If not, click "Cancel". Now select the "Learn Template" button to run the selected rectangle into the program, wait until the button light turns off. Finally click the "Search" button, and an image of the tracking along with an image

of the region of interest should display and track the entire image stack. A file saved as “Analysis” will become available with a file named “Centroid0”. This file contains the results of the bead displacement per pixel with respect to its position in the first image.

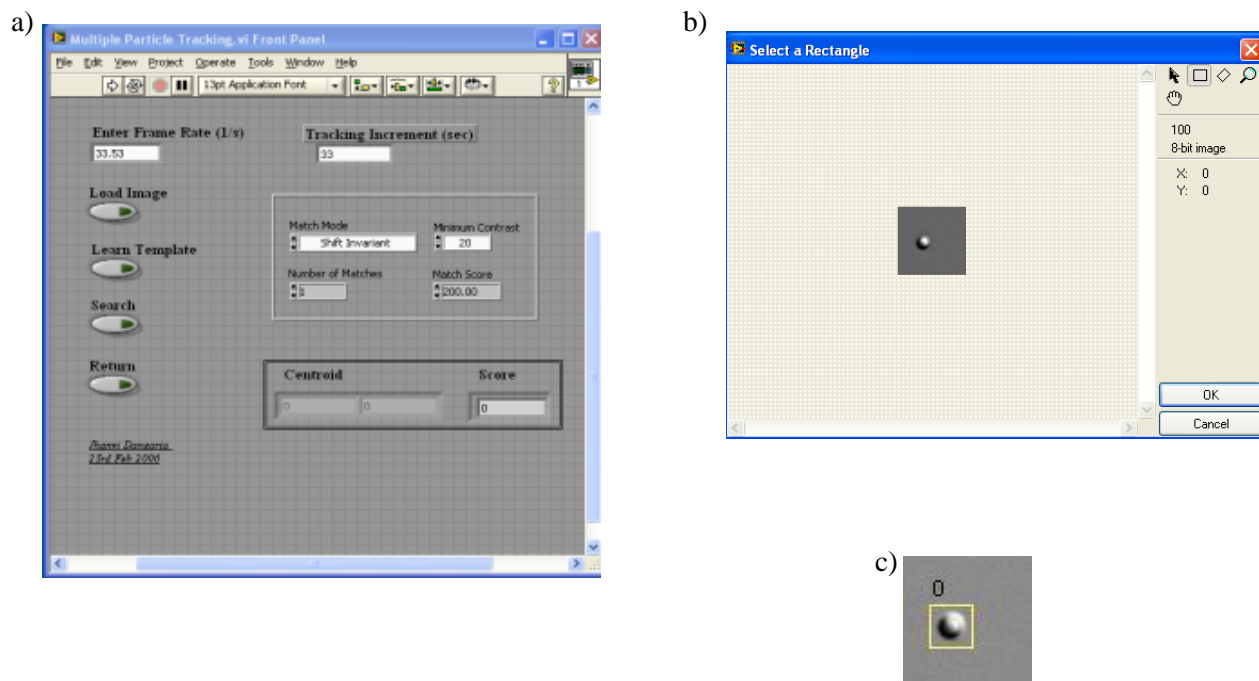


Figure 2-6: Tracking images using LabVIEW software, “Multiple Particle Tracking.vi”. a) The front panel of the VI where the Frame Rate and Tracking Increment are entered. b) The window for selecting the area around the bead to be used as the region of interest. This area is typically a few pixels away from the bead. c) The Region of Interest (ROI) selected around the bead for imaging.

In order to use the results in the “Centroid0” file, the custom LabVIEW program must be used called “MSD vs Tau Main VI.vi”, written by Jhanvi Dangaria. This program converts the pixels displacement to a nanometer scale and saves the data in an Excel file. To use the LabVIEW “MSD vs Tau Main VI.vi”, run the VI and enter the Frame Rate and Tracking Time, the same as used in the program “Multiple Particle Tracking.vi”. Also enter the number of nm per pixel, the default is 100. A new window will pop up for selection of the processing, select “Pre-During-Post”. The file is now converted and labeled “Centroid0” and can be opened up with Excel.

To track the beads with the QPD, two different custom LabVIEW programs called “q4d readout w trigger.vi”, and “Step displacement of nanostage with high rate QPD” were used. Both programs gave readouts of the voltages from the photodiodes in an X and Y direction, as well as a SUM of both the X and Y.

The VI “q4d readout w trigger.vi” was used to compare tracked images of trapped samples with QPD voltage readouts at the same time and rate to be used later for comparison, Figure 2-7.

To operate the LabVIEW “q4d readout w trigger.vi”, run the VI and enter the frame rate and tracking time. This is the same frame rate found on the “Camera Control” and used in the “Multiple Particle Tracking.vi”. The tracking time is the number of frames to be recorded divided by the frame rate. Make sure to always round down this value before entering. A live feed of the QPD voltage readouts will begin scrolling in the graphs. Use the knobs on the steering mirror to move the voltages in the X and Y direction as close to zero as possible. This allows the laser to be centered on the photodiode before recording.

A trigger is used to activate CamWare's record function at the same time as the LabVIEW program records the changes in voltage of the QPD. Set the trigger by opening CamWare => “Camera Control” => Set Trigger. Set “Sequence Start”=>“Triggered” and “Trigger Edge”=>“Rising”. Set CamWare to Record by pressing the red record button and begin recording by pushing the “Trigger CamWare and Data Collection” button in the LabVIEW program. A file is prompted to be saved containing data for each voltage values at the same rate the camera recorded changes in displacement, which may be opened with Excel.

The VI “Step displacement of nanostage with high rate QPD” was used to control the piezoelectric stage, trigger CamWare, and record QPD voltage readouts, Figure 2-7.

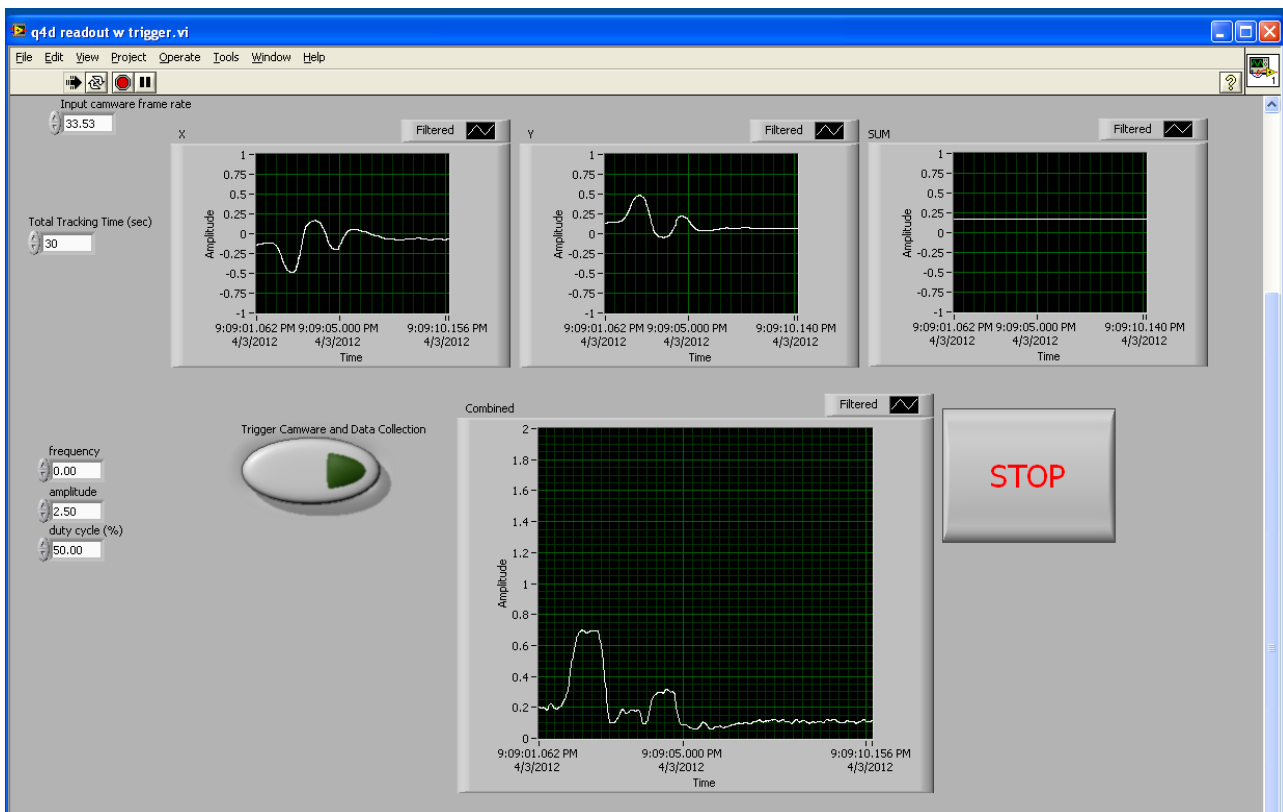


Figure 2-7: Tracking the QPD voltages using “q4d readout w trigger.vi” LabVIEW software. To the left are the values to be entered into the program. Each of the graphs shows the QPD voltage values for the X, Y, and SUM directions, along with a combined graph of both the X and Y values.

To operate the LabVIEW “Step displacement of nanostage with high rate QPD”, run the VI and a window will open to create a folder in which the data will be stored. A live feed of the QPD voltage readouts will begin scrolling in the graph QPD Output. Use the knobs on the steering mirror to move the voltages in the X and Y direction as close to zero as possible. This allows the laser to be centered on the photodiode before. Enter in the time of data collection or Tracking Time. The piezoelectric stage can be moved in increments of 10 μm , 1 μm , 100 nm, and 10 nm in the positive and negative x, y, and z directions. A readout from the stage sensor gives the actual position of the stage.

A trigger is used to activate CamWare's record function at the same time as the LabVIEW program records the changes in voltage of the QPD. Set the trigger by opening CamWare => “Camera Control” => Set Trigger. Set to “Triggered” and “Rising”. Set CamWare to Record by pressing the red record button and begin recording by pushing the “Record Fast QPD after increment?” button and then moving one increment in the x, y,

or z direction. A file is created which contains data for each voltage values at the same rate the camera recorded changes in displacement, which may be opened with Excel.

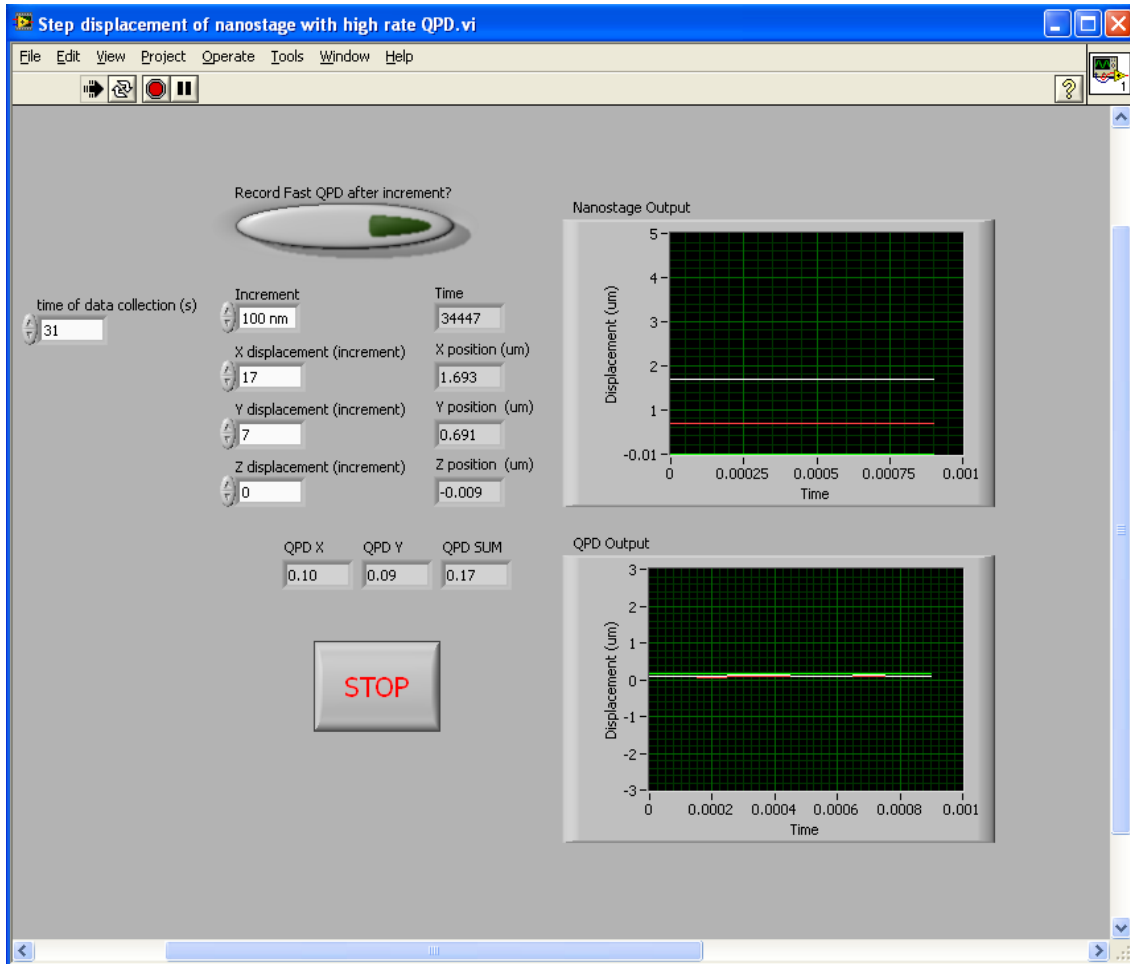


Figure 2-8: Tracking QPD voltages using “Step displacement of nanostage with high rate QPD” LabVIEW software. To the left are the values to be entered into the program. On the right are graphs indicating the piezoelectric sensor output for the stage’s displacement in the x, y, and z direction in nanometer increments and the QPD output for the X, Y, and SUM voltages.

Chapter 3

Methods

Spring Constant

The results of the CCD camera's image displacements were analyzed by taking the difference of each value to find the change in displacement between each frame as $X_1 - X_2 = X_{\text{displacement}}$, rather than the displacement in reference to the first image. This was done for all frames in both the X and Y axes. The RMS was taken of all values of displacement giving an average displacement in both the X and Y axis; X_{RMS} and Y_{RMS} . These values were then entered into the Equipartition Theorem equation, $U = \frac{1}{2} k_{\text{spring}} x^2 = \frac{1}{2} k_{\text{boltz}} T$ where U is the potential energy, k_{spring} is the spring constant, k_{boltz} is the Boltzmann constant, and T is the temperature at which the experiment occurred. Through this $k_{\text{spring,x}}$, $k_{\text{spring,y}}$, and $k_{\text{spring,xy}}$ values are obtained. The optical trap is estimated to have a spring constant of about 11 pN/micron. Therefore, the trap spring constant is on the same order as that of the expected force production for bead displacements of about 0.5 μm .

Attaching Beads to the Coverslip

A dual ligand (DL) system of biotinylated fibronectin was used to bind avidin coated polystyrene beads ($\sim 2\mu\text{m}$) to the coverslip. This DL system used the high affinity of avidin-biotin binding (Figure 3-1) with lower affinity fibronectin. This is similar to Anamelechi's use of streptavidin-biotin bonding to adhere cells to polymers, except for these applications the avidin coated bead is substituted for streptavidin coated cell (Anamelechi et al., 2007)

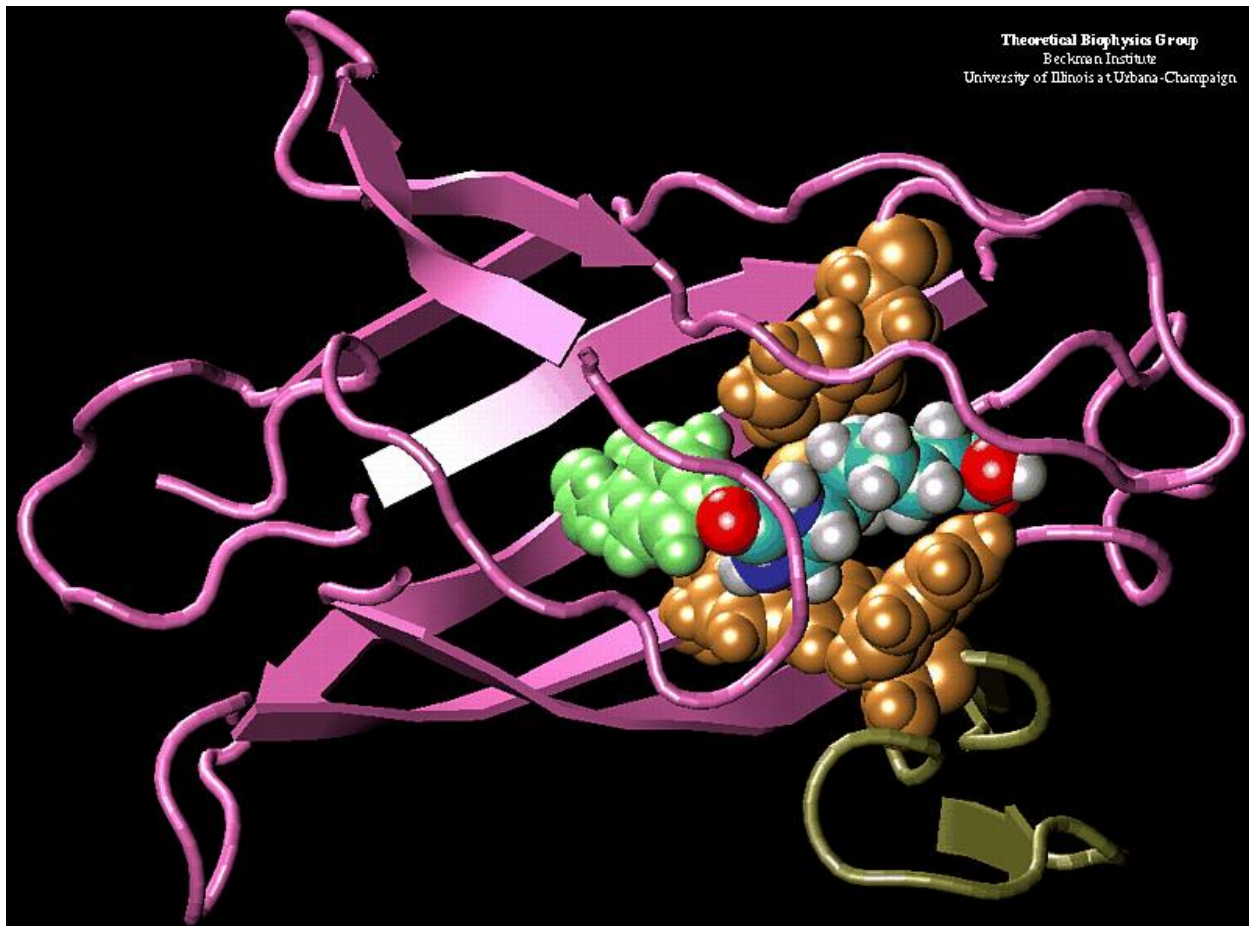


Figure 3-1: Image of avidin and biotin binding. In this image the purple protein with brown and green bonding sites is avidin and has a “cup” shape. The multicolored protein is biotin. (Izrailev, 1997)

Biotinylation of fibronectin was accomplished using with Sulfo NHS-LC-Biotin. A solution of FN (1mg/mL) was mixed with 8mM Sulfo NHS-LC-Biotin dissolved in ultrapure water for 30 min at room temperature. The cover slip was bound with the above solution of biotinylated fibronectin (bFN). A 50 μ L sample of bFN was pipetted onto the surface of a sterile cover glass bottom culture dish (Delta T dish Black from Biotecth). The bFN was incubated at room temperature for 45 min. The remaining solution was aspirated and rinsed with Dulbecco's Phosphate Buffer Solution (DPBS). One thousand μ L of DPBS was added to the culture dish to prevent the coating from drying and to prepare a solution that the avidin coated beads could be suspended in.

The beads float through the DPBS to the surface of the culture dish (or are trapped and dragged) and bind to the bFN coated surface. Once the bead are bound there was little to no movement, and the bead could not be removed with the aid of the optical trap.

Calibration of the Quadrant Photodiode

Two separate methods were used to calibrate the QPD, the first method used 1 μm polystyrene beads suspended in water; the other used the DL system of avidin coated beads bound to the cover slip.

The QPD was calibrated using the change in voltage values of the QPD against the camera's change in displacement values. The laser beam going to the QPD was adjusted using the adjustment mirror so that the voltage values read near zero for both the QPD's X and Y direction. Then the LabVIEW program "q4d readout w trigger.vi" was run so that voltage values were recorded at the same rate that the camera recorded images. It should be noted that the QPD's X and Y direction is at a ~ 45 degree angle to the stage's and the image's X and Y direction. Therefore the values of the change in voltage could not be directly compared to the changes in displacement. Instead the variance of the changes in voltage were found and compared to the changes in displacement. This was repeated for different trap heights above the cover slip in the Z direction, beginning where the bead was in contact with the cover slip to 15 μm above the cover slip in 5 μm intervals.

The second method used a bFN coated culture dish with an avidin coated bead floating down and binding to the surface. The optical trap was moved to a position 2 μm away from the bead's edge and data was taken as the piezoelectric stage was moved in 100 nm increments in a specific axis until the trap had passed through the bead, ending up 2 μm beyond the bead's edge, for a total path of ~ 6 μm (2 μm on each side of the bead, 2 μm for the bead itself). This allowed the bead to be moved through the trap as QPD and imaging data were taken simultaneously (using the LabVIEW program). As soon as the stage moved both the QPD data and the CamWare began recording for 10 seconds, with the QPD at 30,000 Hz and the CamWare at 25.05 Hz. As the bead moves through the optical trap, it bends the laser light of the trap, which is picked up on the QPD. In most QPD applications the laser is reflected on a small portion of the QPD, see Figure 3-2, any change is the laser position

would still result in the same QPD SUM as the intensity of the beam remains the same, see Table 3-1. However in this application, it is possible that the laser light and the QPD are close to the same size, the QPD being 1 mm, and the laser light projected beam diameter just under 1 mm (although future work needs to be done to verify the size of the beam on the QPD). This means that any change in the laser position would affect the amount of laser light on the QPD, which has the potential of greatly changing the intensity of the laser and therefore the QPD's SUM, while at the same time making the sensors in the x and y direction of the QPD very sensitive, see Figure 3-2. This will be used to compare the bead's position with the output voltage of the QPD.

Table 3-1: Equations for QPD voltage readout

QPD Coordinate	Equation
X Coordinate	$S_x = (V_2 + V_4) - (V_1 + V_3)$
Y Coordinate	$S_y = (V_1 + V_2) - (V_3 + V_4)$
SUM (Z Coordinate)	$S_{SUM} = V_1 + V_2 + V_3 + V_4$

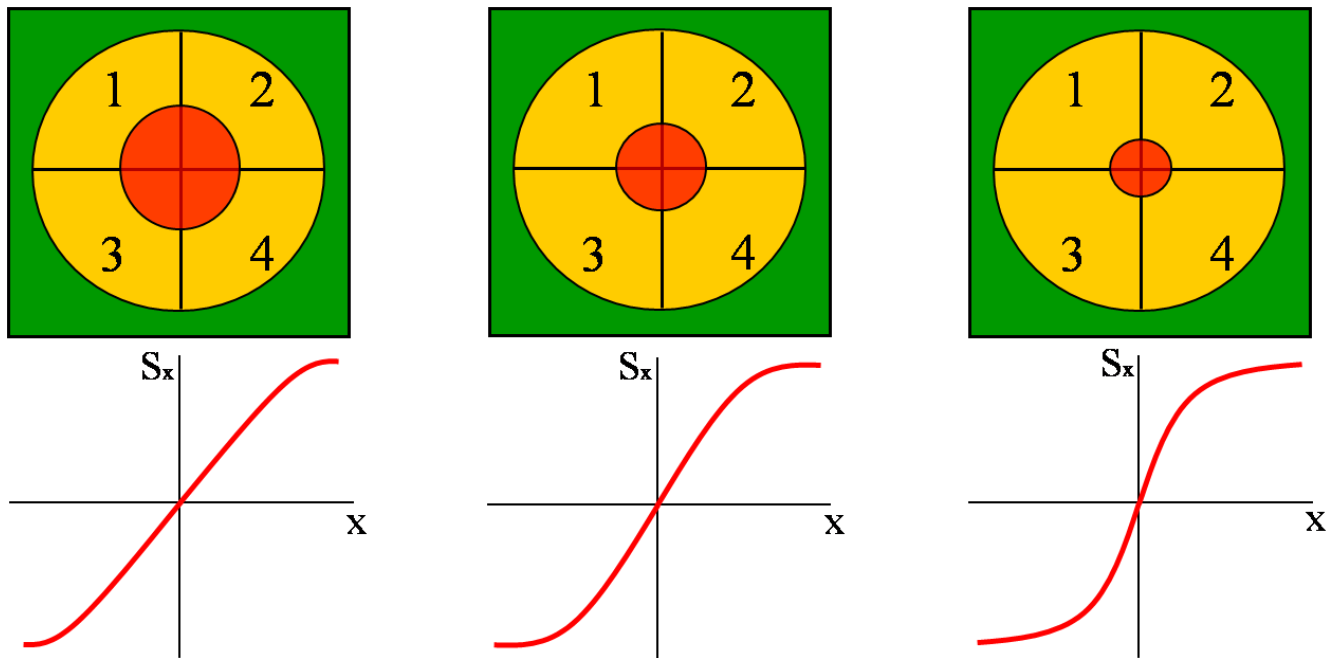


Figure 3-2: Laser on QPD. As the laser beam increases in diameter the SUM remains the same ($S_{SUM} = V_1 + V_2 + V_3 + V_4$). However, the X and Y voltages become less sensitive to change as the beam size increases ; i.e. the slope of the linear region (Montes-Usategu).

Detection of Single Binding Events

This method used a bFN culture dish to trap an avidin coated bead by bringing it down to the cover slip and measuring the avidin-biotin reactions. In this method, modeled after Jeney et al (Jeney, 2010) molecules of avidin coated on beads are bound to a coverslip coated with biotinylated fibronectin. $2\mu\text{L}$ of bead solution was added to the culture dish at a time to a maximum of $4\mu\text{L}$. The bead was initially moved $\sim 2\mu\text{m}$ above the cover slip, and the piezoelectric stage was raised in the +z direction (so that the top of the coverslip would intersect the focal point of the trap) in 100 nm increments, using the LabVIEW program “Step displacement of nanostage with high rate QPD.vi” The idea behind this is as the stage gets closer to the trapped bead, eventually it will reach a point where Brownian motion will move the bead so close to the bFN surface of the cover slip that the attached avidin will bind to the biotin of the bFN. At this point, the number of avidin-biotin bindings will increase and any more bead motion will be inhibited. In short the bead will “jump” and “stick” to the cover slip, Figure 3-2. Using

a known spring constant k_s , and displacement (x_e) of the bead due to the binding reaction, we can find the force F of the reaction ($F = k_s * x_e$).

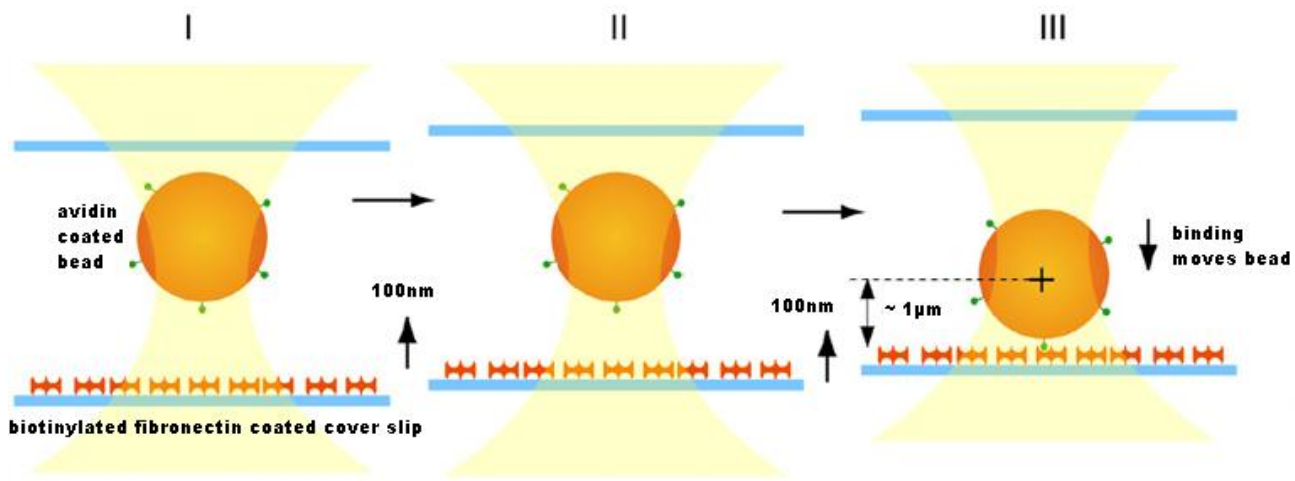


Figure 3-3: Bead coated with avidin, surface coated with biotinylated fibrinogen. As the cover slip is moved in the + z direction in 100 nm increments, it finally comes so close that the biotin bind to the avidin; immobilizing the bead. (Jeney, 2010)

During this time both the CCD camera and the QPD will be recording the reaction. Once the bead binds to the surface, the imaging will give us visual confirmation of the time the reaction occurred. Since not all of the avidin-biotin bindings will occur at the same time, it is expected that the QPD data can be analyzed to determine the individual reactions taking place which will occur in steps. We expect that the first bond will result in loss of z-motion, the second bond, should restrict components of lateral motion, and a third bond should restrict almost all motion.

Bead Binding to Cells

This final experiment will be an application of the previous “Binding Force Measurement” experiment to live cells. This will be performed by attaching the bFN to the avidin coated beads, 50 μM of bFn are injected into a 50 μM sample of beads and incubated for 45 minutes. Ideally, the beads should be centrifuged and rinsed to prevent excess bFN from entering the experiment and attaching to the cells. However, this was not done in order

to prevent bead aggregation. A sample of bovine aortic endothelial cells was prepared and placed on the coverslip and 4 μL of bead solution was pipetted in. A bead was trapped, placed in contact with the surface of the cell, and held there for 100 seconds (1.6 minutes). The surface proteins (β_1 integrins) on the cell's membrane are expected to interact and bind with the fibronectin attached to the bead, which inhibits the bead's movement. It would be very difficult to recognize this with the imaging of the CCD camera; however data from the QPD should give evidence of limited bead movement. This data can be compared to the limited movement of the bead by the "bead on coverslip experiment" to demonstrate the validity of this experiment.

Results & Discussion

Beads at Different Distances from Surface of Coverslip

Polystyrene beads of $1\ \mu\text{m}$ were trapped above the coverslip in a solution of water and their positions were recorded for 30 seconds at varying heights from the cover slip from 0 to $15\ \mu\text{m}$ in $5\ \mu\text{m}$ increments. As the beads were moved away from the coverslip it became evident that the spring stiffness decreased initially right above the coverslip and increased afterwards up to $15\ \mu\text{m}$, Figure 4-2a-b. It is hypothesized that the decreased spring stiffness directly above the coverslip is due to the bead bouncing off the coverslip from Brownian motion. At $15\ \mu\text{m}$ above the coverslip, the beads became unstable in the trap and were easily lost. It is believed that as the bead moved further away from the coverslip the laser intensity decreases and the trap becomes weaker.

Figure 4-1: Calibration of optical trap at different distances from surface,

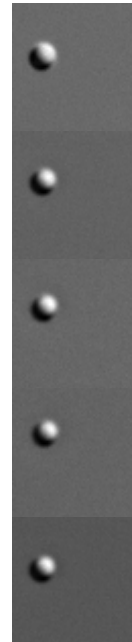
(a) on cover slip,

(b) just above cover slip $\sim 100\ \text{nm}$,

(c) $5\ \text{nm}$ above cover slip,

(d) $10\ \text{nm}$ above cover slip.

(e) $15\ \text{nm}$ above cover slip.



When comparing the spring stiffness to the QPD data we can see that the variances of the voltages are consistent with the spring stiffness, see Figure 4-2c. Although there is little movement of the bead when the bead is at the coverslip, there is a high average variance of the QPD voltages. It is suspected that this may be due to interference from the coverslip as diffraction between the coverslip and bead may occur. As the height from the cover slip increases the QPD variance decreases, this result is expected because as the spring stiffness increases the bead has less movement in the x and y directions. Less bead movement would mean that there is less laser movement and therefore a smaller variance in the QPD voltages. However, most objectives are corrected for spherical aberrations only close to the coverslip. Spherical aberrations should reduce the trap strength. Thus, we expected that the trap strength would decrease with increasing distance from the coverslip. But this is not what we observed. It is possible that the correction collar on the objective was not adjusted properly for the coverslips that were used because it was not easy to measure them (due to the walls of the chambers). Future work will be required to address this discrepancy.

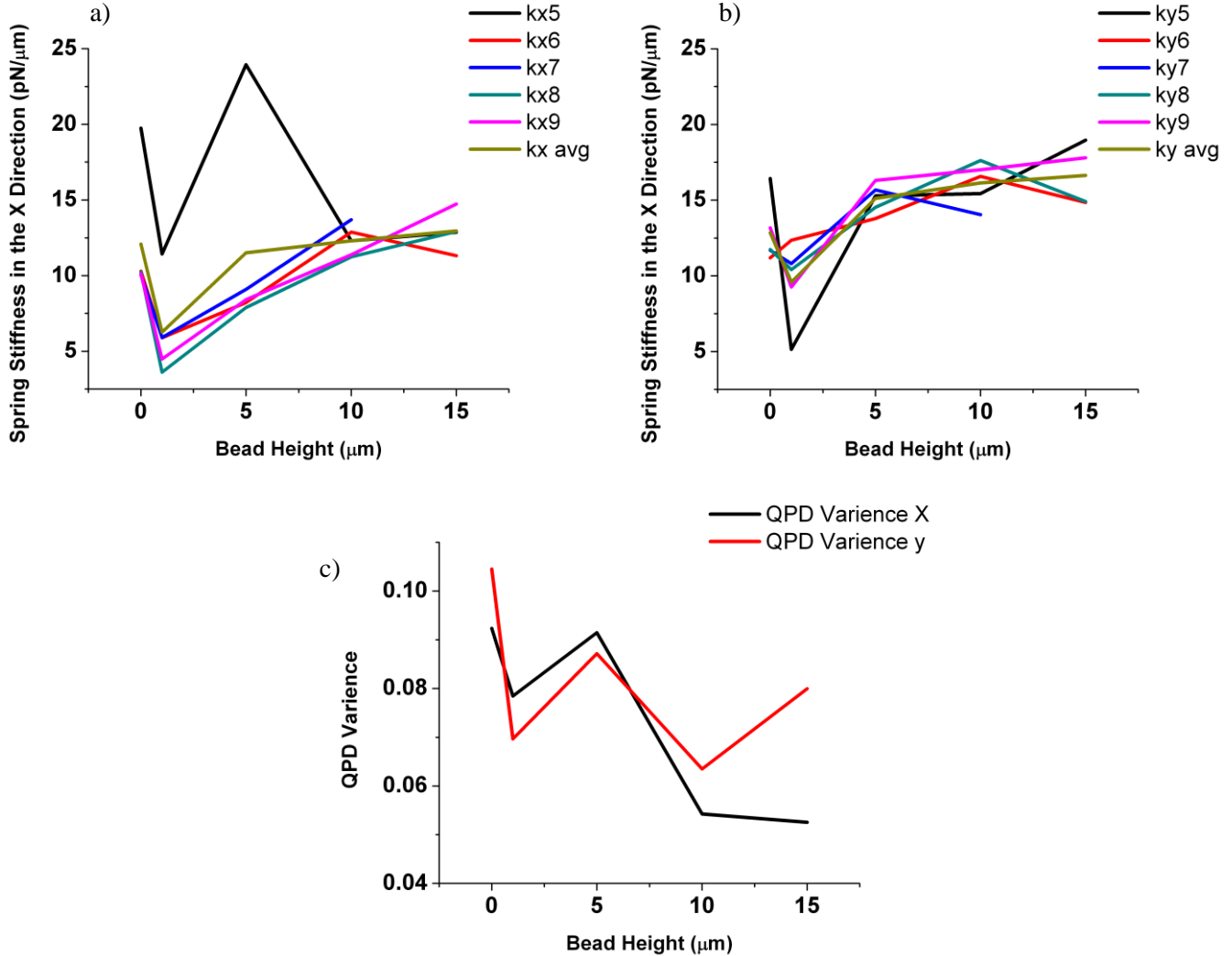


Figure 4-2: Spring stiffness and QPD variance vs. bead height. a) The spring stiffness in the X direction vs. bead height, the average maximum spring stiffness was measured to be ~ 12 pN/ μm at 15 μm above the cover slip. b) The spring stiffness in the Y direction vs. bead height, the average maximum spring stiffness was measured to be ~ 17 pN/ μm at 15 μm above the cover slip. c) The average variance of the QPD voltage values for the bead at varying heights. Generally as the spring stiffness increases the QPD variance decreases.

Calibration of the Quadrant Photodiode

A 2 μm avidin coated bead was bound to the surface and moved through the laser trap both 2 μm before and after the bead using the piezoelectric stage, Figure 4-3. Data was taken only for the X and Y directions.

Figure 4-3: Bead moving in X direction

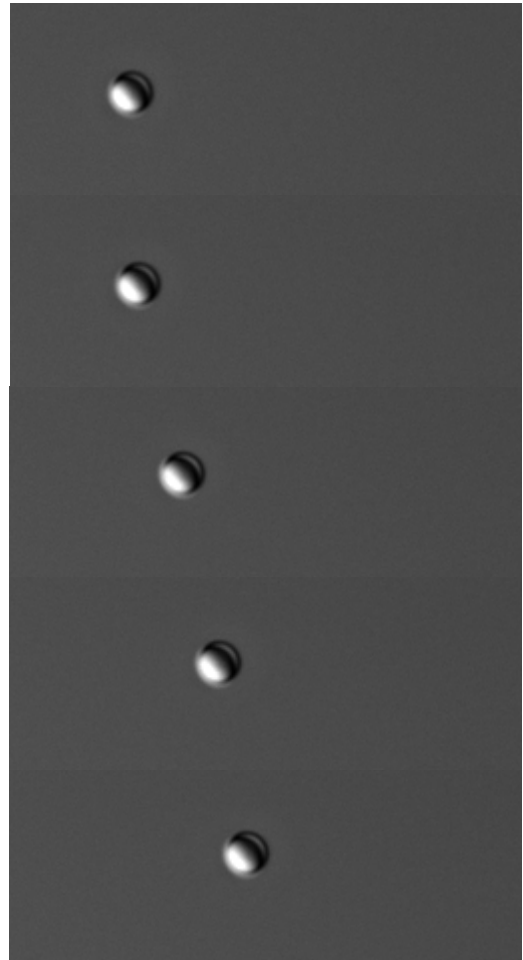
At frame 1, starting position of bead

At 1000 frames, 0.4 μm

At 7000 frames, 2.8 μm

At 12000 frames, 4.8 μm

At the final 16000 frames, 6.4 μm



The beads movement was recorded simultaneously with the CCD camera (Figure 4-4) using CamWare and the resulting laser movement with the QPD, (Figure 4-5) using “Step displacement of nanostage with high rate QPD.vi”.

The image was converted to a series of stacks and run through the LabVIEW Program “Multiple Particle Tracking” using a 42 X 42 pixel region of interest. The results of the imaging show that the bead does move at a uniform rate. However, notice how the recorded movement is not uniform at each movement in Figure 4-4d, instead there seems to be some backward movement before each change in position and the change in position is less than the expected 100 nm from the piezoelectric sensor readout. The backward movement may be due to the piezoelectric stage, but it is unlikely because the QPD readout always recorded longer then the CamWare image

recordings. It is more likely that this is an issue with the CamWare software or the LabVIEW software used to process the particle tracking. Not including the backward movement, it was found that the average X_{RMS} and Y_{RMS} for the bead during the stationary period was 2.894 nm and 3.201 nm respectively. This means that the stationary portions can be considered relatively stable and any movement is due to mechanical noise.

For future work imaging should be taken with the filter wheel on the microscope at “Position 5” where both the bead and the laser can be viewed at the same time. This will allow for visual confirmation of the bead entering the trap to compare to the changes in QPD voltages.

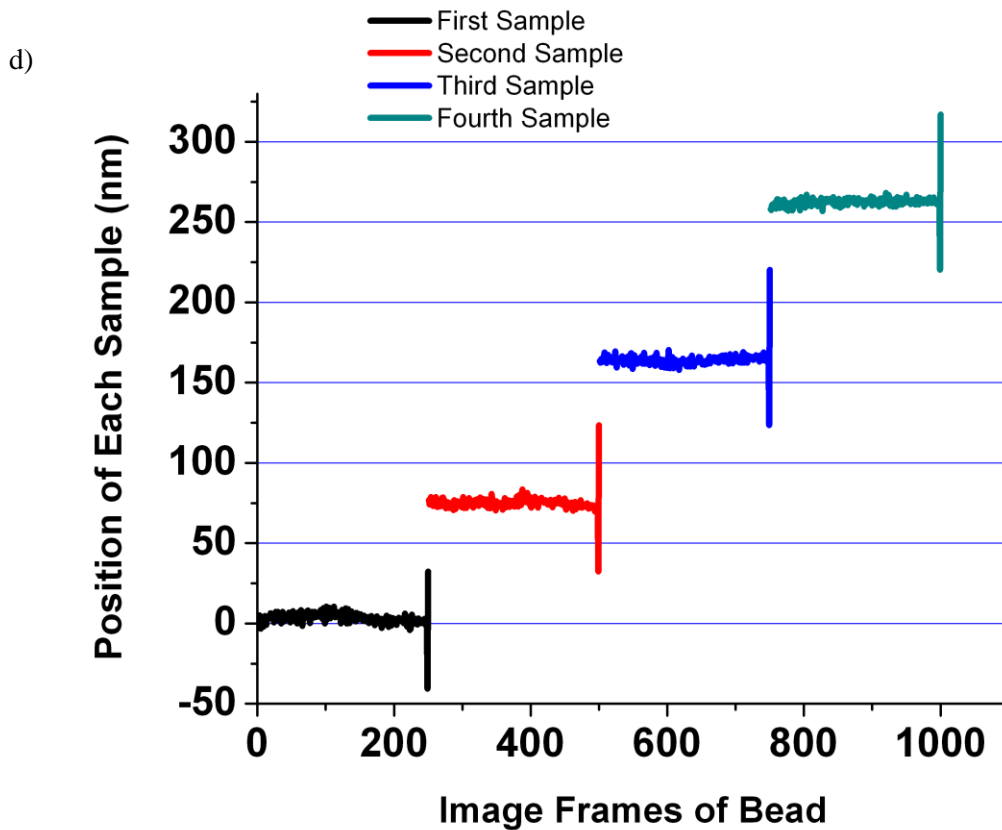
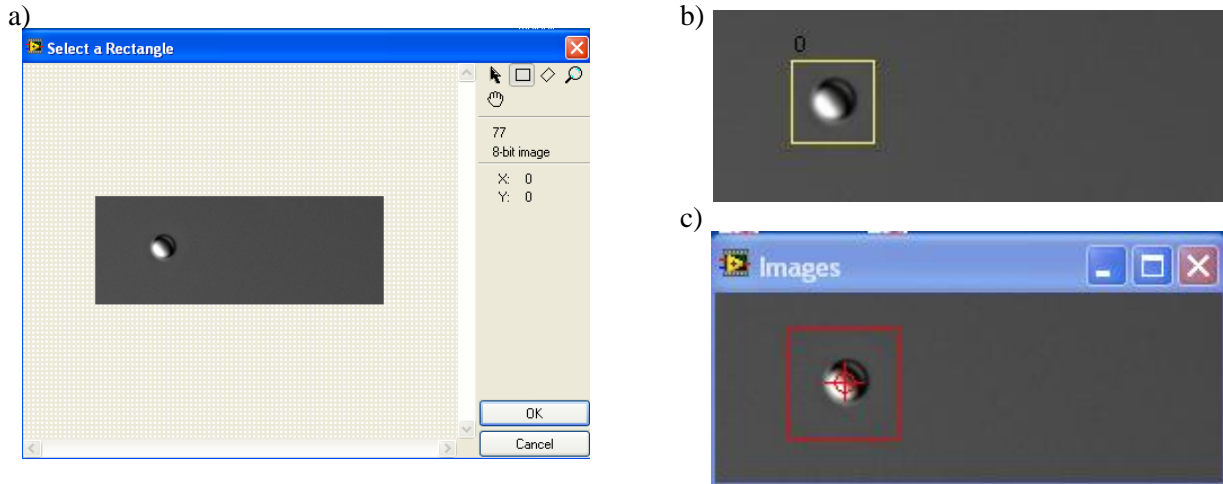


Figure 4-4: Tracking of imaged bead in X direction using tracking LabVIEW program. a) The first file of the stack of the imaged bead b) A 32 pixel by 32 pixel region of interest is selected around the bead c) The tracking image while the program analyzes the changes in frames d) Graph of the position of each sample vs. the image frames of the bead as it was moved in the X direction for the first four recordings. Each sample is 250 frames, taken for 10 seconds. There is exhibited some backward movement at the end of each sample recording. The change in position is also less than the expected 100 nm from the piezoelectric sensor readout.

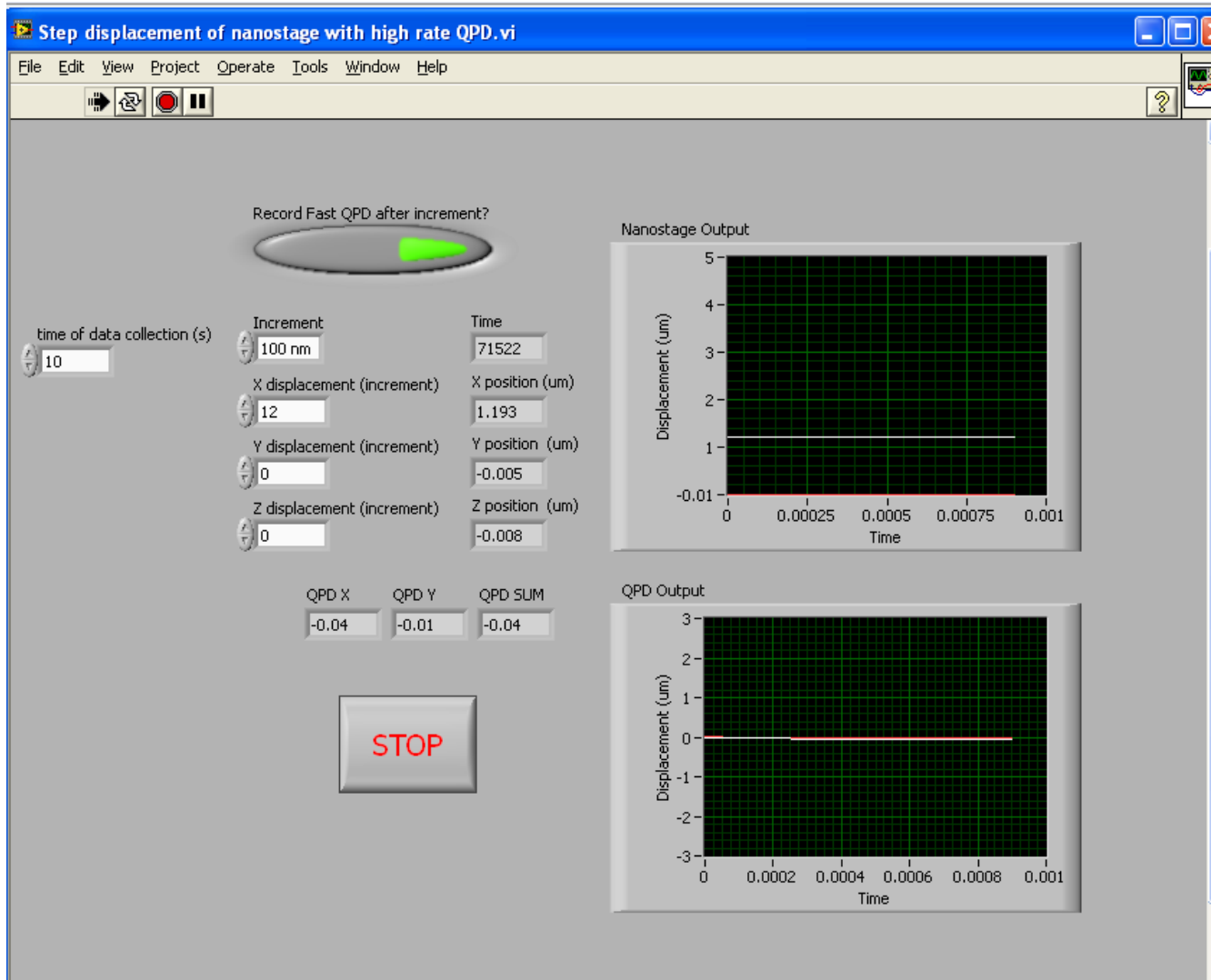


Figure 4-5: Tracking of imaged bead in X direction using QPD and stage sensor

In order to confirm that the stage movement from the piezoelectric motors is occurring at the expected intervals, the stage sensor readouts are compared to the bead's tracked position, (Figure 4-6). This should result in a linear graph with a slope of 1, with both axis having relatively similar values. Although the trend line is linear, it has a slope of approximately 0.92. It can be seen that the average position obtained from image-based tracking is consistently less than the positions sensed by the stage sensor. A reason for this discrepancy could be that an

assumption made with the tracking software of the conversion of pixels to nanometers, with each screen pixel on screen at a length of 100 nm. If this was increased then the image position would better compare to the stage readout position. Another possibility is that the stage is moving less than the expected amount, even though the stage sensor readout is giving the expected amount. For future work the length of each screen pixel should be recalculated to rule out the first possibility as the second one would require an entirely new stage to ensure proper data processing and results.

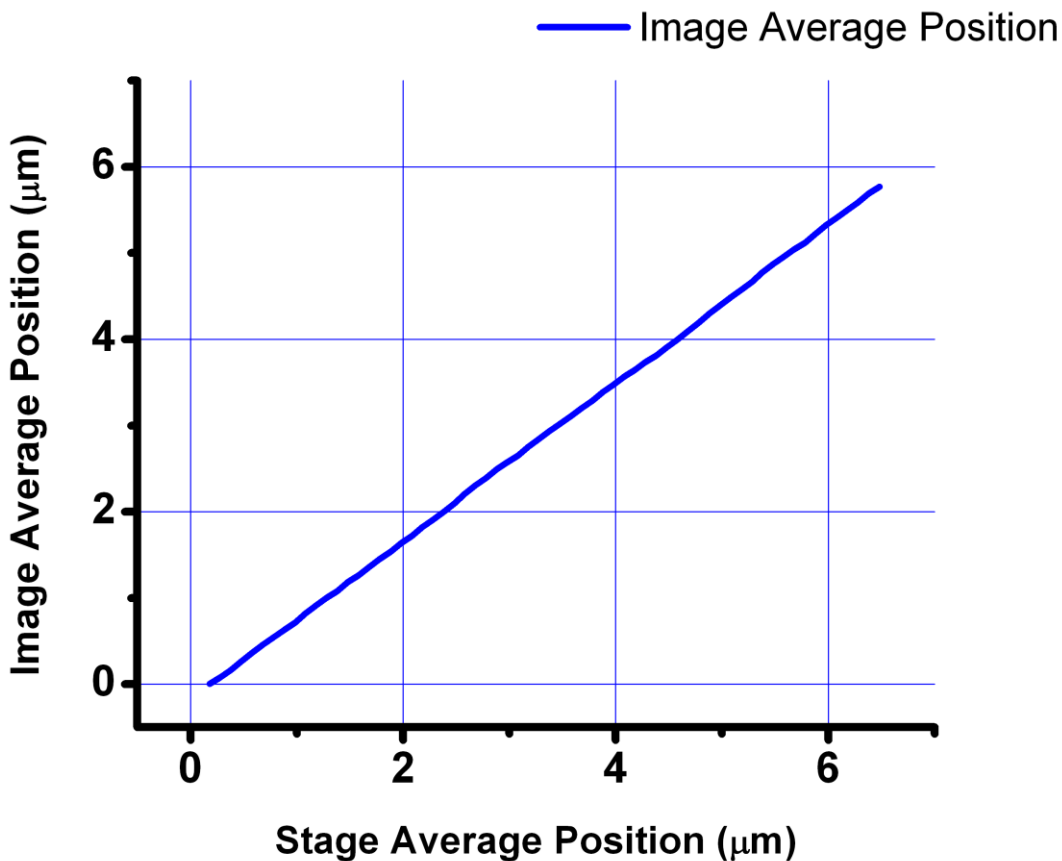


Figure 4-6: Graph of x axis average QPD readout (µm) versus tracking software position (µm), notice how each Image average position is less than the Stage average position for the same sample taken.

The results of the QPD voltages while the bead was moved show that there is a correlation between movement of the bead through the trap and QPD voltage levels. In Figure 4-7a an example of the output voltages for movement in the X direction is shown. Notice before the bead comes into contact with the focal point of the

trap around point 24, both the X axis and Y axis exhibit the same waveform in opposite directions. It is hypothesized that this is caused by interaction of the diffraction patterns from the laser with the bead as it moves. This is also seen after the bead leaves the focal point of the trap after point 53. It should also be noted that at position 39, where the bead should be at the center of the trap, the X voltage exhibits a change in direction with a zero voltage readout at about the center position. The Y does not exhibit a zero voltage readout, but it should be noted that in this region there is a dip in voltage. It is hypothesized that this is due to the laser being centered on the QPD when the bead is in the center of the focal point.

It is interesting to note the SUM component only changes during the points of 24 through 53. It can be seen that the SUM has a slight decrease from points 24 to 31 and a slight increase in points 47 to 53. It is hypothesized that as the edge of the bead moves into the trap, the projection of the laser beam on the QPD shifts off of the QPD and decreases the voltage sum. As the bead is moved into the center of the trap, the laser passes through and is evenly distributed across the QPD. Finally, as the edge of the bead moves out of the trap the position of the laser moves again and increases the beam intensity. To support this hypothesis evidence should be seen of a clear correlation between the voltages in the X and Y Axis. Although there does seem to be some evidence of correlation, there is no clear distinction, and this could be caused by a slight misalignment of the projected beam on the QPD. More tests in the future need to be conducted to determine the precise size of the projected laser beam on the QPD and to determine the effect of the orientation of the QPD, which is at 45° relative to the stage coordinates.

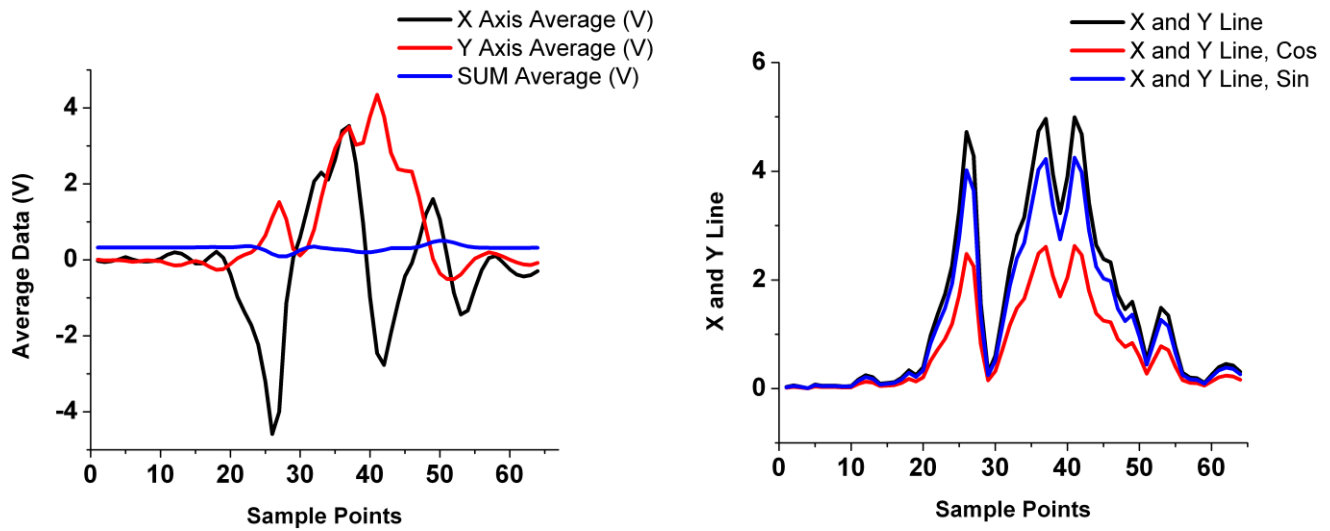


Figure 4-7: Graphs of x-axis calibration for QPD. a) The average X, Y and SUM voltage outputs from each sample point. The raw data can be viewed in Appendix B. b) A graph of the voltage scalar at each point calculated as the square root of the sum of X^2 and Y^2 multiplied by either the sine or cosine of 45°

This evidence shows the bead has an estimated 29 positions where it interacted with the trap ($53 - 24 = 29$). If it is assumed that the bead is $2 \mu\text{m}$, then it would take 20 positions (at 100 nm per position) to travel though the first point where it interacts with the trap. However the bead must travel an additional distance to move completely through the trap. The trap distance is estimated to be the wavelength of the laser, $\sim 830 \text{ nm}$, or on the order of $1 \mu\text{m}$. This would mean the bead should take about 30 positions to travel though the entire trap. The result of 29 positions of interaction with the trap seems to make sense. Using this information the position where the bead is in the center of the trap can be estimated, about position 39. This also gives evidence that the QPD sensors are giving correct readouts, and that the length of each screen pixel should be re-calculated for the conversion of pixels to nanometers.

It is known that the X and Y axis of the QPD is at an approximate 45° angle from the stage's X and Y Axis. This angle arises because of the way the QPD is mounted on the internal circuit board and the way the housing of the QPD is anchored to the microscope. This makes it difficult to compare movement of the stage to a voltage change in the QPD. In this experiment, when the stage moves in the X direction the voltages change in the QPD in both the X and Y direction. If we try to combine the X and Y voltage outputs as vectors using the Pythagorean

Theorem: $X \text{ and } Y \text{ Line Output} = \sqrt{(X \text{ voltage})^2 + (Y \text{ voltage})^2}$, we get a voltage scalar which should be at the maximum value when there is the greatest change in voltages; when the bead crosses the trap beam, see Figure **4-7b**. In order to try and derive the X and Y components from the scalar, the equation was multiplied by $\cos(45)$ and $\sin(45)$, respectively; X component of X and Y Line Output = $\sqrt{(X \text{ voltage})^2 + (Y \text{ voltage})^2} * \cos(45)$, and Y Component of X and Y Line Output = $\sqrt{(X \text{ voltage})^2 + (Y \text{ voltage})^2} * \sin(45)$, as seen in Figure **4-7b**. Although the evidence does not seem to give anything dramatic about the X and Y components, the overall X and Y Line Output presents maximums which correlate to points where the bead is entering and exiting the trap, and where the bead is in the center of the trap, at position 39.

In Figure **4-7b** an example of the output voltages for movement in the Y direction is shown. Not such a thorough analysis of the Y axis data will be given as the X axis, but similarities will be highlighted. The bead comes into contact with the laser's focal point around point 25, and leaves the focal point at around point 54. Both the X and Y axis exhibit a waveform in opposite directions before and after the contact with the laser. This supports the hypothesis that this is caused by interaction of the diffraction patterns from the laser with the bead. It should also be noted that near position 40, where the bead should be at the center of the trap, both the X and Y voltage are exhibits a maximum. It is hypothesized that this is due to the laser being centered on the QPD when the bead in in the center of the focal point.

It is interesting to note that once again, the SUM component only changes during the few points after the bead edge enters the trap and right before the final bead edge leaves the trap. This supports the hypothesis that as the edge of the bead moves into the trap, the position of the laser moves and increases the intensity certain photodiodes slightly. In this case it was to influence the negative photodiodes each time. There also seems to be evidence of correlation between the X and the Y axis. As the X axis voltage decreased, the Y axis seems to follow suit but in the negative direction. More tests in the future should be considered.

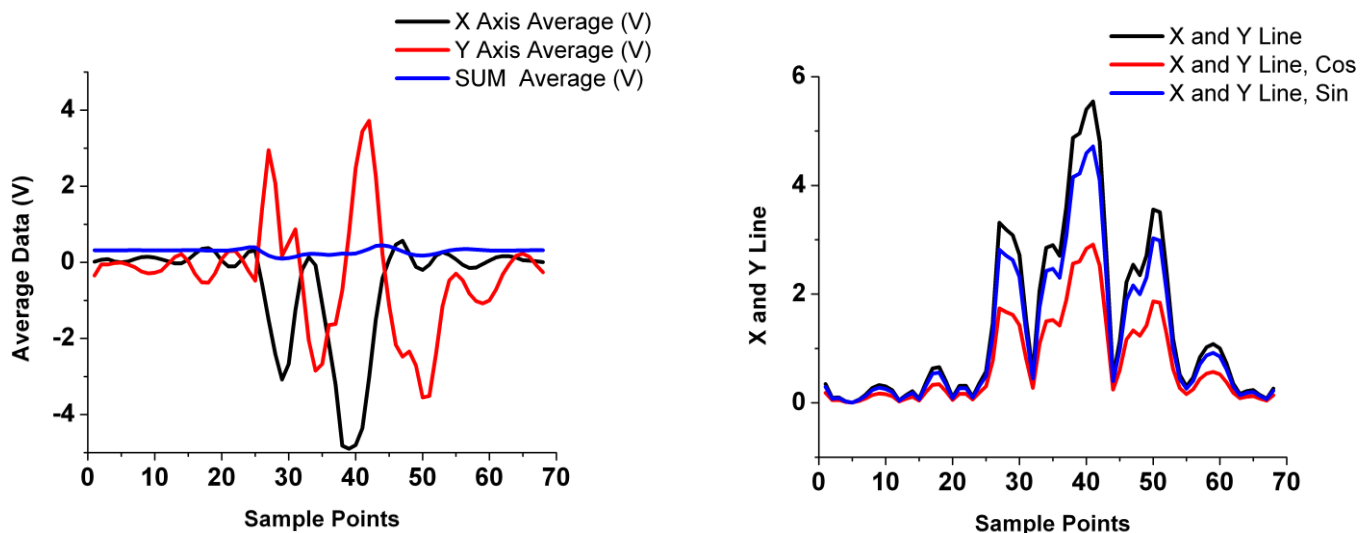
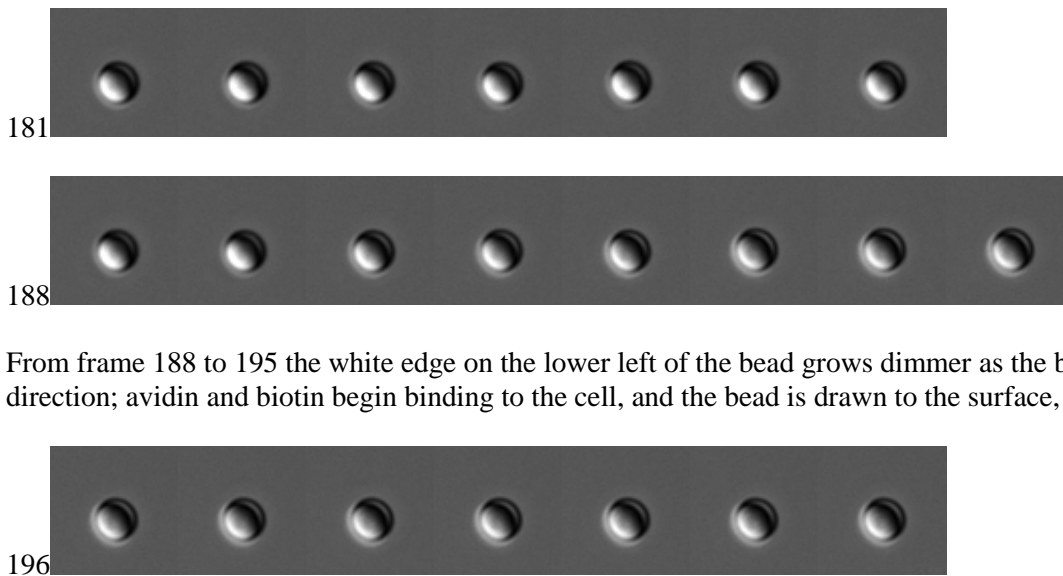


Figure 4-8: Graph of y-axis calibration for QPD a) The average X, Y and SUM voltage outputs from each sample point. The raw data can be viewed in Appendix B. b) A graph of the voltage scalar at each point

The X and Y voltage outputs are combined using the Pythagorean Theorem: X and Y Line Output = $\sqrt{(X \text{ voltage})^2 + (Y \text{ voltage})^2}$, and the X and Y components are found from the scalar by multiplying the equation by $\cos(45)$ and $\sin(45)$ respectively, Figure 4-8b. Once again, the evidence does not seem to give anything dramatic about the X and Y components. The X and Y Line Output presents maximums which correlate to the points where the bead is entering and exiting the trap, and where the bead is in the center of the trap. This could be used in the future to determine the bead position from QPD data.

Detection of Single Molecule Binding Events

In this experiment, the bead was lowered to the coverslip in 100 nm increments, and bound to the coverslip as predicted, providing images with a dramatic binding event and QPD voltage changes. A small amount of movement by Brownian motion can be measured, but as soon as the bead binds it moves from the focal point of the trap to the coverslip. This is confirmed visually with the change in shading of the bead (Figure 4-9).

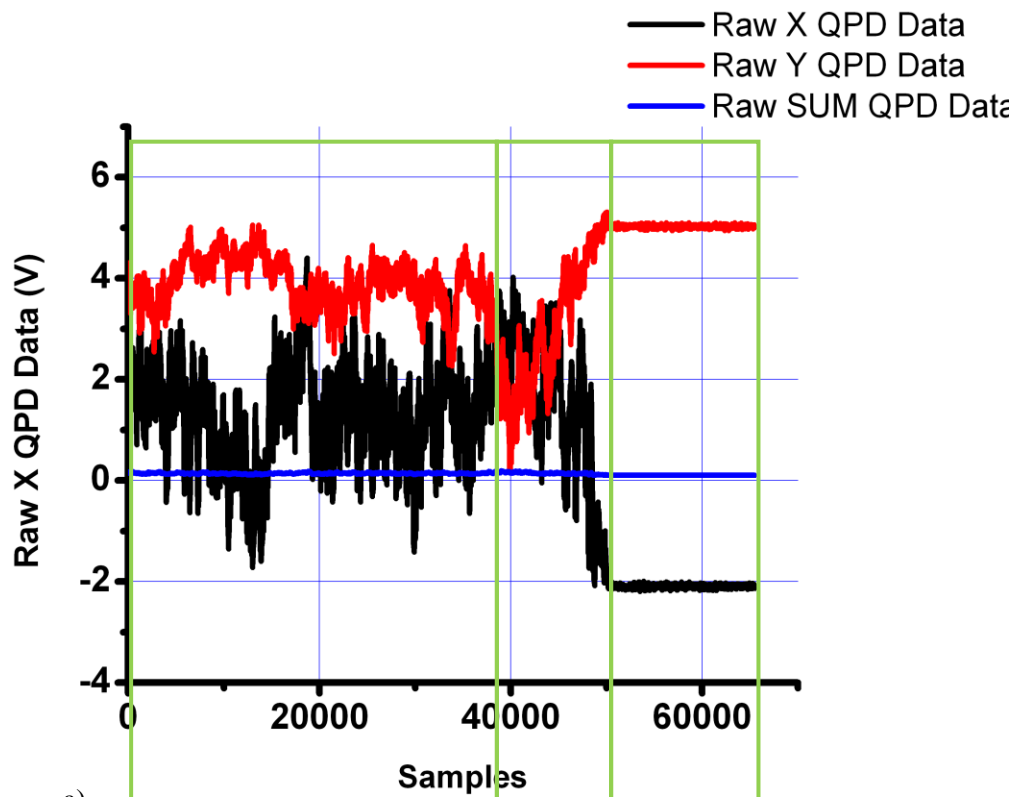


From frame 188 to 195 the white edge on the lower left of the bead grows dimmer as the bead moves in the -z direction; avidin and biotin begin binding to the cell, and the bead is drawn to the surface,

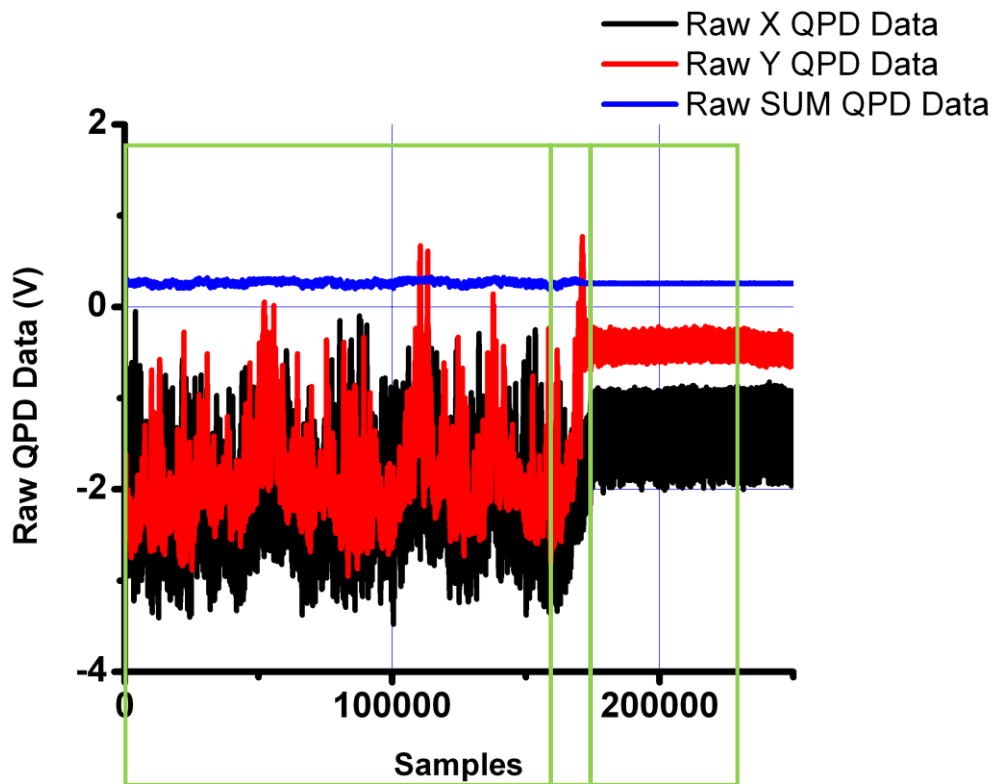
After frame 195, there is no movement and the bead image does not change.

Figure 4-9: Bead coming close to bFN surface using optical trap 181 Images 181-187 are typical bead movements when a bead is trapped.

The QPD data was taken using the LabVIEW program “Step displacement of nanostage with high rate QPD.vi” at a rate of 30000 samples/s for 30 seconds. Upon viewing the QPD data, there is a large amount of movement during the beginning of the recording, so much so that it looks like noise. When the binding event occurs, there can be seen a series of step-like voltage changes from the QPD, (Figures 4-10). Each binding reaction limits bead movement; it is hypothesized that that each step represents a binding action of biotin to avidin as the bead binds and then moves to one side and is bound by another protein, until the bead is completely immobilized. This staggered bead movement would explain the steps seen on the QPD. After the binding event the QPD voltage reading stabilizes and does not change significantly for the remainder of the recording.



a)



b)

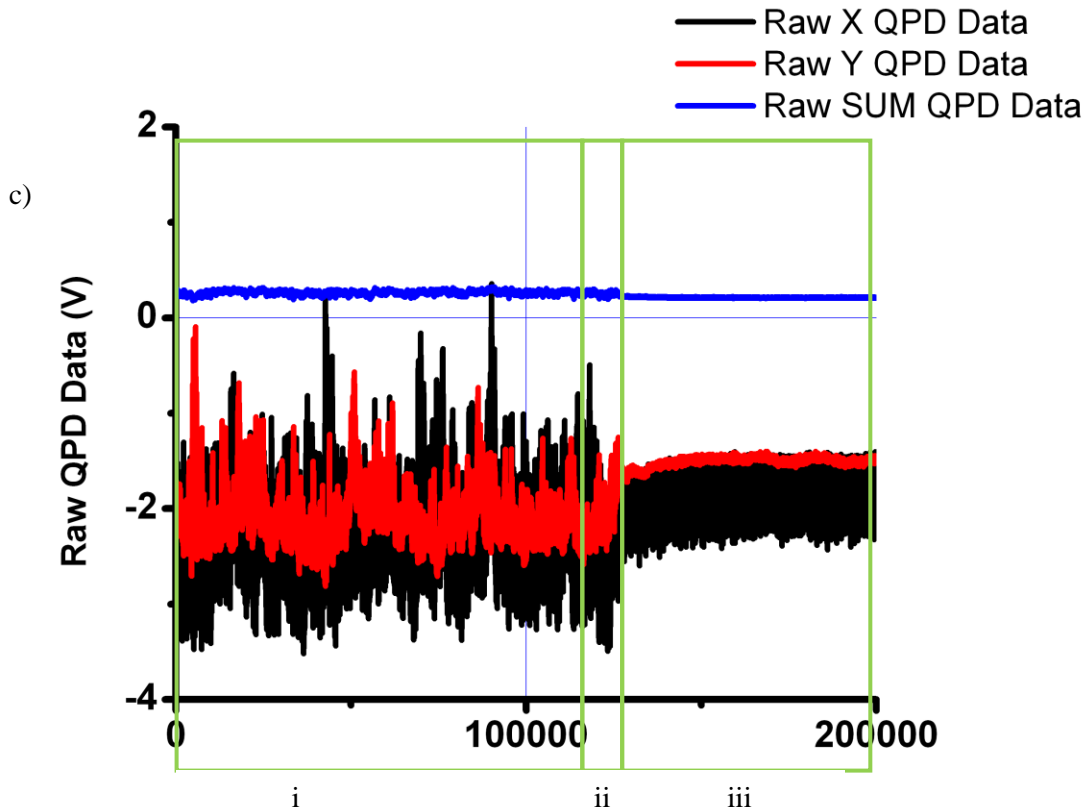


Figure 4-10: Raw QPD data, displaying rapid adhesion to a biotinylated fibronectin coated cover slip. Each image is split up into three parts; i) Before the binding event, ii) The step-like voltage change while the avidin and biotin complexes bind, iii) The stabilized bead after the binding event.

- a) i) The before binding event lasted about 39,000 samples or ~1.3 seconds. ii) The binding event recorded with just over 10,000 samples, or about 0.33 seconds in real time. iii) The QPD readout has the least noise of any of the samples, with little to no movement of the bead.
- b) i) The before binding event lasted about 160,000 samples or ~5.3 seconds. ii) The binding event recorded with just over 10,000 samples, or about 0.33 of a second in real time. iii) The QPD readout has more noise in the X axis than in the Y, this may be caused by the bead not being completely immobile and a small amount of noise due to Brownian motion.
- c) i) The before binding event lasted about 115,000 samples or ~3.8 seconds. ii) The binding event recorded was also just over 10,000 samples, or about 0.33 of a second in real time. iii) The QPD readout has more noise in the X axis than in the Y, this may be caused by the bead not being completely immobile.

Using the QPD data between each of the steps of the binding reaction, it can be estimated how fast the binding reactions occurred (< 1 sec) as well as how far the bead moved from the center of the trap to the immobilized position on the coverslip. Using the spring stiffness of the beam and the displacement of the bead,

the force generated at each step could be estimated using a Hookean spring equation: $F = k_{spring} x$. In order to obtain this calculation, future calibrations of the relationship between QPD voltage and bead displacement need to be made.

Bead Reactions with Bovine Aortic Endothelial Cells

In this experiment, a fibronectin-coated bead was trapped and lowered to a bovine aortic endothelial cell grown on the cover slip. When the bead was placed on the cell, its placement was confirmed visually with the CCD camera, (Figure **4-11**), but it could not be determined visually if there was any change in movement. The QPD data was taken using the LabVIEW program “Step displacement of nanostage with high rate QPD.vi” at a rate of 10000 samples/s for 100 seconds. Examining the data, there is not a dramatic binding event as in “Detection of single molecule binding events”, but there are several instances where potentially the bead’s movement was inhibited by formation of focal adhesions, (Figure **4-12**). To determine a binding event there must be a decrease in movement of the bead, and therefore less variation in the QPD voltages. Examples of possible binding events are outlined in Figure **4-12**.

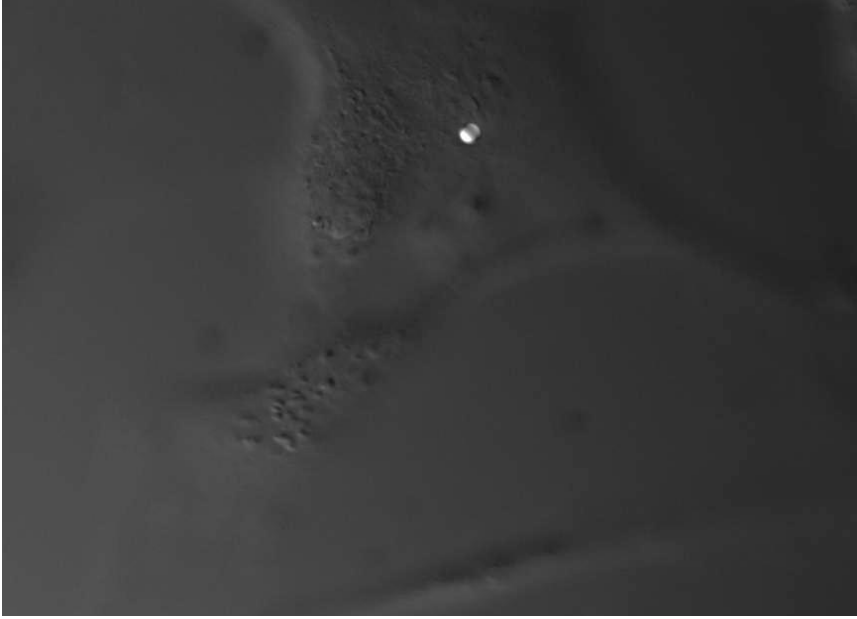
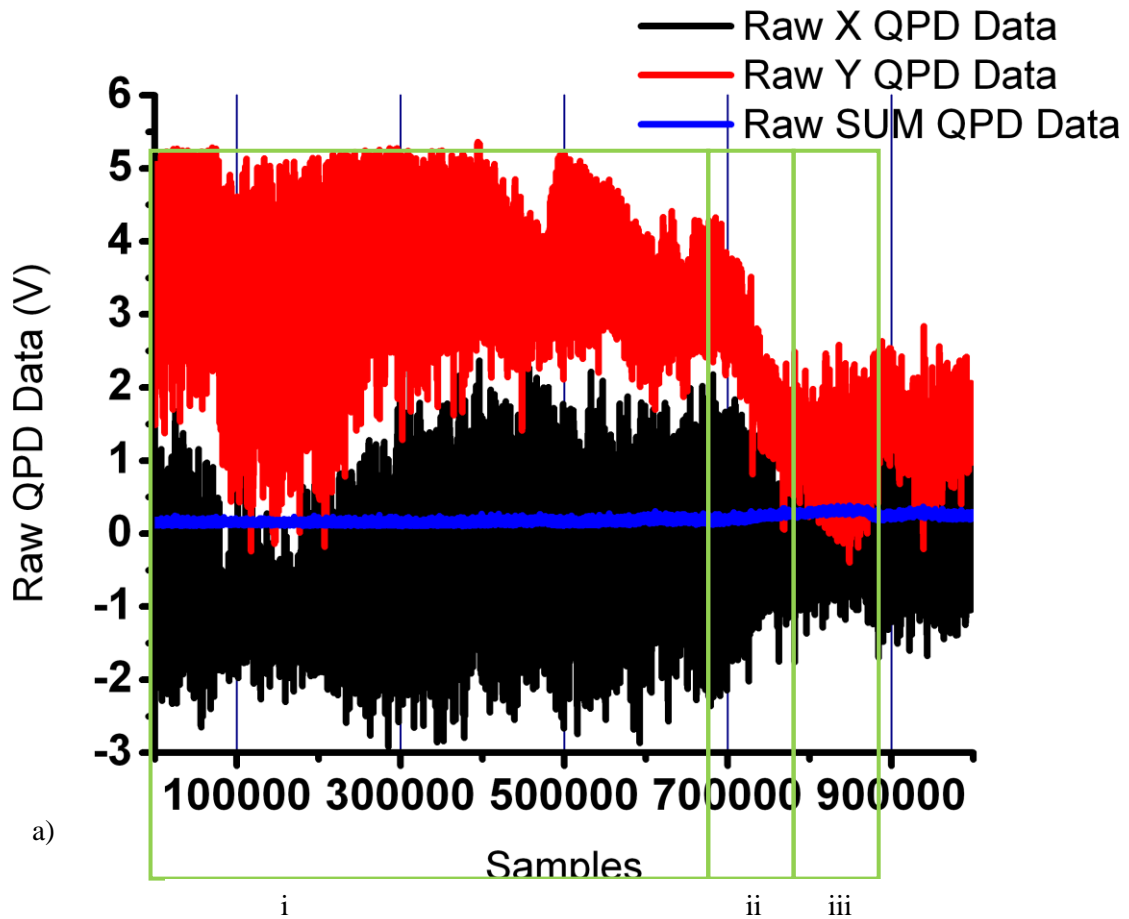


Figure 4-11: Fibronectin coated 2 μm bead held in place on the bovine nerve cell surface using optical trap



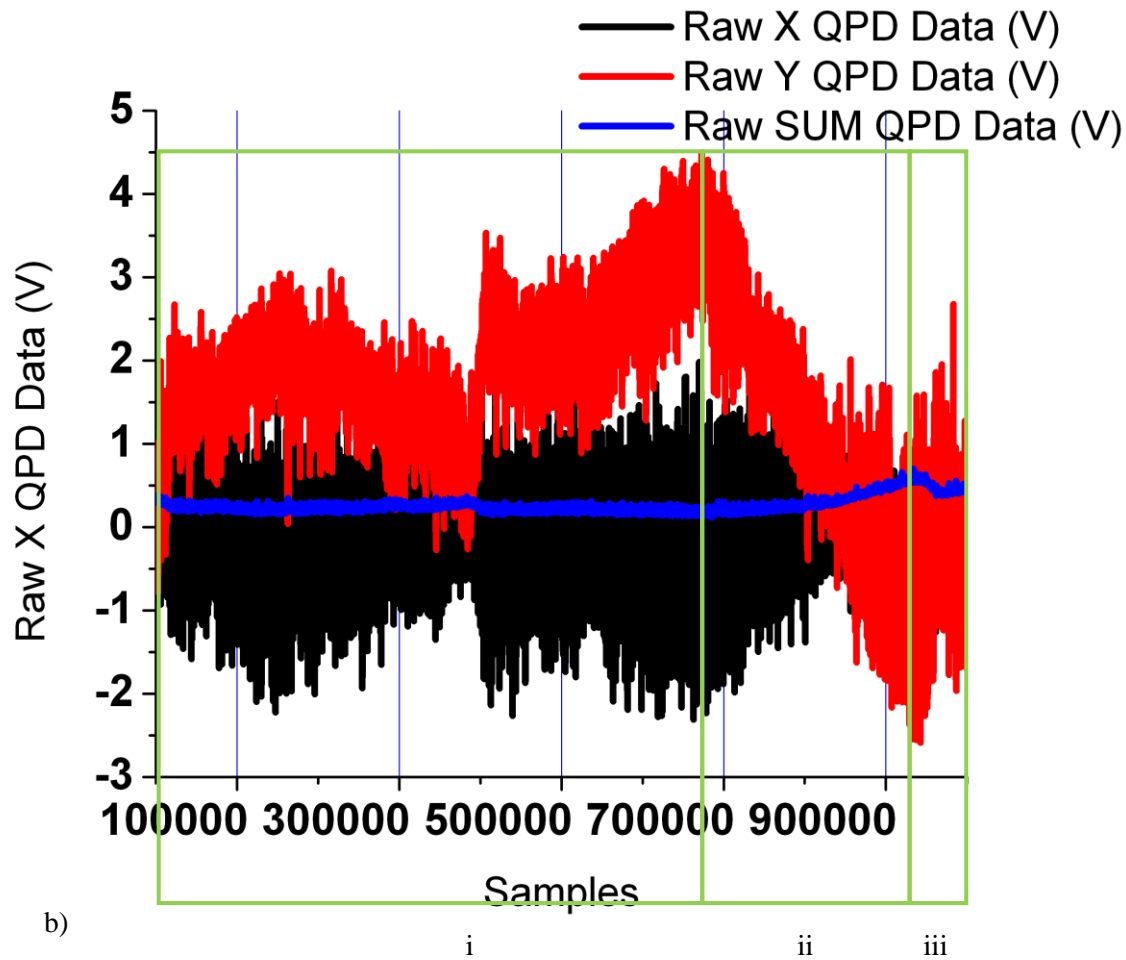


Figure 4-12: Raw QPD data, displaying focal adhesion formation by bovine aortic endothelial cell induced by fibronectin coated bead. It is difficult to determine exactly where binding events occur, there may be several binding events in this data sequence, this examination focuses on ones which are most evident.

- a) i) There may be binding events at 400,000 and 500,000 samples, but the most evident is just after 680,000 samples or 680 seconds. ii) It is estimated that a binding event occurs in this sample series because the Y axis voltage dramatically decreases, the X voltage increases slightly, and the SUM voltage begins a steady incline for the first time during this sampling. The binding event occurred in about 50,000 samples, or about 5 seconds. iii) The QPD readout voltages remains relatively constant as though the bead's movement is inhibited until about 890,000 samples. At this point all of the voltages drastically change and the SUM voltage drops for the first time after the gradual incline. This may be due to a movement of the cell or unbinding of the proteins by some unknown force or chemical means.
- b) i) There may be binding events at 200,000 and 600,000 samples, but the most evident is again around 680,000 samples or 680 seconds. ii) It is estimated that a binding event occurs in this sample series because the Y axis voltage again dramatically decreases, the X voltage increases slightly, and the SUM voltage begins a steady incline for the first time during this sampling, becoming more evident after 900,000 samples. The binding event occurred for about 250,000 samples, or about 25 seconds. iii) After about 920,000 samples the QPD readout voltages drastically change and the SUM voltage drops for the first time after the incline. This may be due to a movement of the cell or unbinding of the proteins by some unknown force generated by the cell.

When the examples of binding reactions with cells are compared to the “Calibration of the QPD” and the “Binding Force Reaction Experiment”, there are several similarities which strongly suggest that a focal adhesion reaction or series of reactions has occurred. In the “Calibration of the QPD” it is shown that the QPD X and Y voltages change dramatically when the bead moves, and the SUM voltage only changes when an edge of the bead is moved close to the trap center. It can be hypothesized that Figures **4-12 aii** and **bii** are evidence of the bead being displaced from the trap center. In the “Binding Force Reaction Experiment” during the binding events (Figure **4-10 aii, bii, and cii**) there is a step-like voltage changes which may indicate the binding action of biotin to avidin and the displacement of the bead as it binds. These step-like voltage changes occur in Figures **4-12 aii** and **bii** and may indicate focal adhesion of the fibronectin to cellular integrin molecules and bead displacement. Using the QPD data between of the binding reaction, it could be estimated how fast the binding reactions occurred (5-25 seconds) as well as how far the bead moved from the center of the trap. At this time displacement of the bead cannot be estimated, and this must be left up to future work.

Conclusions

Conclusions

This thesis examined aspects of the optical trap including setup, calibration, and experimental applications with biologically relevant research. This document can be used as an instruction manual for the next student who works in the Mechanotransduction Laboratory. Effective use of the optical trap gives insight into the understanding the piconewton forces and nanometer displacements produced during binding reactions and focal adhesions. Measurement of spring constants of the bead at different height from the cover slip gave an understanding of the spring constants involved with the trap. Analysis of the Quadrant Photodiode calibration showed there is a correlation between the bead movement and the changes in voltage in the X and Y axes as well as the SUM. Binding of the bead to the coverslip and to bovine aortic endothelial cells demonstrated that binding events could be observed with the Quadrant Photodiode and in future work the force of these reactions can be determined. Further studies need to be conducted with this system to create a program for the Quadrant Photodiode to be comparable to nanometer displacements in three dimensions.

References

- Anamelechi, C. C., Clermont, E. E., Brown, M. A., Truskey, G. A., & Reichert, W. M. (2007). Streptavidin binding and endothelial cell adhesion to biotinylated fibronectin. *Langmuir*, 23(25), 12583-12588.
- Aufderheide KJ, Du Q, Fry ES. Directed positioning of micronuclei in *Paramecium tetraurelia* with laser tweezers: absence of detectable damage after manipulation. *J Eukar Microbiol*. 1993;40:793-796.
- Cheezum, M. K., Walker, W. F., & Guilford, W. H. (2001). Quantitative comparison of algorithms for tracking single fluorescent particles [Abstract]. *Biophysical Journal*, 81(4) 2378-2388.
- Chen, H., Ge, K., Li, Y., Wu, J., Gu, Y., Wei, H., et al. (2007). Application of optical tweezers in the research of molecular interaction between lymphocyte function associated antigen-1 and its monoclonal antibody. *Cellular & Molecular Immunology*, 4(5), 221-225.
- Chen, W., Zarnitsyna, V., Sarangapani, K., Huang, J., & Zhu, C. (2008). *Measuring Receptor–Ligand binding kinetics on cell surfaces: From adhesion frequency to thermal fluctuation methods* Springer New York. doi:10.1007/s12195-008-0024-8
- Conia J, Voelkel S. *Optical manipulations of human gametes*. *BioTechniques*. 1994;17:1162-1165.
- Davidson, M. W. (2009). *Introduction to microscope objectives*. Retrieved 4/02, 2012, from <http://www.microscopyu.com>

- Gelles, J., Schnapp, B. J., & Sheetz, M. P. (1988). Tracking kinesin-driven movements with nanometre-scale precision. *Nature*, 331(6155), 450-453.
- Izrailev, S., Stepaniants, S., Balsera, M., Oono, Y., & Schulten, K. (1997). Molecular dynamics study of unbinding of the avidin-biotin complex. *Biophysics Journal*, 72(4), 1568-1581.
- Jeney S, Stelzer E H K, Grubmuller H and Florin E L 2004 *ChemPhysChem* 5 1150–8
- Keen, S., Leach, J., Gibson, G., Padgett, M., Keen, S., Leach, J., et al. (2006). Comparison of a high-speed camera and a quadrant detector for measuring displacements in optical tweezers. *JOURNAL OF OPTICS A-PURE AND APPLIED OPTICS*, 9, 264-266.
- Kuo S C and Sheetz M P 1993 *Science* 260 232–4
- Mark C. Williams. (2002). Optical tweezers: Measuring piconewton forces. In P. Schuille (Ed.), *Single molecule techniques* (Biophysics Textbook Online ed.,)
- Molloy J E, Burns J E, Kendrick-Jones J, Tregear R T and White D C S 1995 *Nature* 378 209–12
- Montes-Usategu, M., et al.
Back-focal-plane interferometry. Retrieved April 02, 2012, from <http://sites.google.com/site/bioptub/force-detection/back-focal-plane-interferometry>
- Muddana, H. S., Sengupta, S., Mallouk, T. E., Sen, A., & Butler, P. J. (2010). Substrate catalysis enhances single-enzyme diffusion. *Journal of the American Chemical Society*, 132(7), 2110-2111. doi:10.1021/ja908773a
- Neuman, K. C., & Block, S. M. (2004). Optical trapping. *Review of Scientific Instruments*, 75(9), 2787-2809. doi:10.1063/1.1785844

Stout, A. L. (2001). Detection and characterization of individual intermolecular bonds using optical tweezers.

Biophysics Journal, 80(6), 2976-2986. doi:10.1016/S0006-3495(01)76263-7

Sun, G., Zhang, Y., Huo, B., & Long, M. (2009). *Surface-bound selectin–ligand binding is regulated by carrier*

diffusion Springer Berlin / Heidelberg. doi:10.1007/s00249-009-0428-y

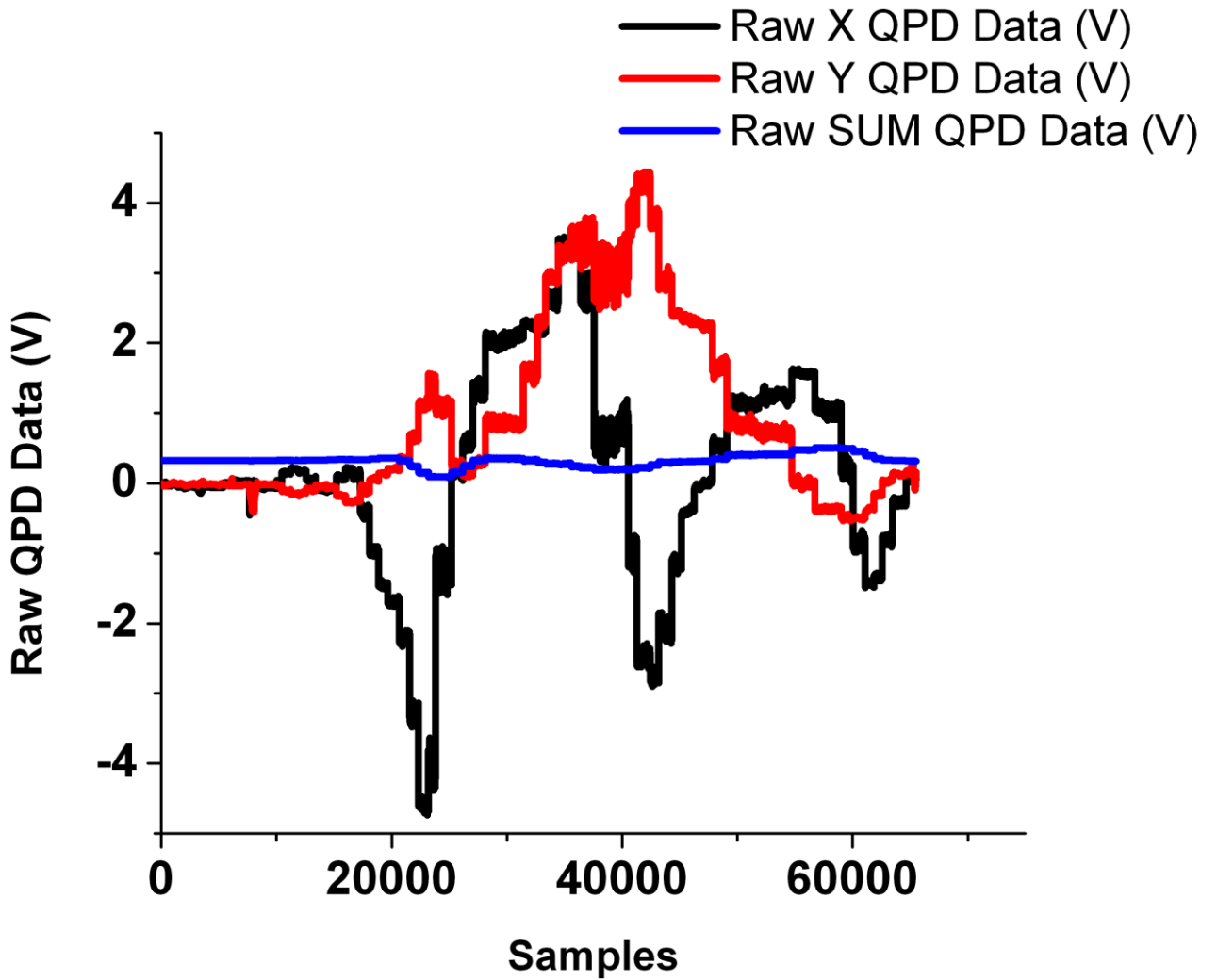
Vorobjev IA, Liang H, Wright WH, Berns MW. Optical trapping for chromosome manipulation: a wavelength

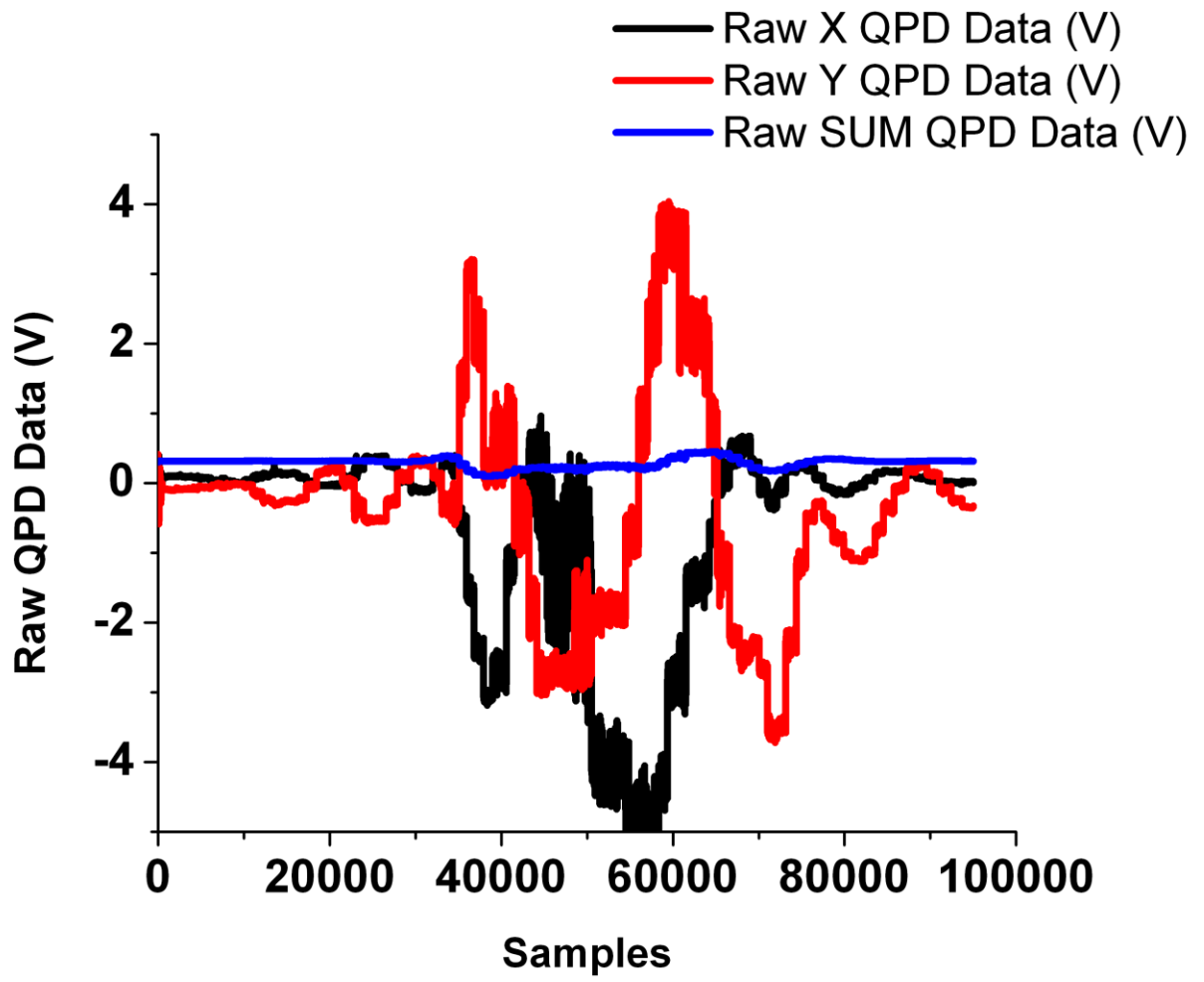
dependence of induced chromosome bridges. *Biophys J*. 1993;64:533-538.

Appendix A

Raw Data Images

Below are graphs of raw X-axis and Y axis calibration for the QPD. These correspond to Figure 4-8 respectively.





Appendix B

Readme Instruction File: Directions for Particle Tracking

Instruction for finding the k (spring value) of the optical trap laser

PARTICLE TRACKING

The main VI (Multiple Particle Tracking.VI) is in the Multiple Pattern Matching folder.

Step 1:

Enter: Frame rate (Frames per second in Hz?)
Tracking increment (# of frames/frame rate = total time in seconds)
NOTE: automatically rounds to greatest whole number

Example ?

Frame rate: 30 fps
Tracking Increment: 10 seconds

Step 2a:

Convert file to 8-bit in ImageJ, (comes 16-bit from camera "SensiCam QE, Cooke").
In Image J go to Image=> Type=> 8-bit.
Save in new folder: Save As=> Image Sequence=> Format TIFF
This unstacks the images, so each frame is an individual file

Step 2b:

Run the VI
Press 'Load Image'
Find the location of image dataset (See Step 2a)
Select 1st image

Step 3:

Image window will pop-up. Select a ROI (draw rectangle around particle of interest)
NOTE: must draw around entire particle (bead) don't leave edges out, use Zoom
Feature
Press OK
Image window will pop-up again. Select additional ROI's. (not needed for single
bead)
If ROI selection is done, press Cancel.

Step 4:

Press 'Learn Template' wait till green light goes off.

Step 5:

Press 'Search'. The program automatically tracks each of the selected particles one by one.

Step 6:

Once tracking is complete press 'Return' to end program.

Note:

This program saves original and trajectory maps in jpg format. Analysis folder will be created in the same folder as your test images.

ANALYSIS

main VI: MSD vs Tau Main VI

Step 1:

Enter resolution: 123 nm/pixel (default)
Frame rate: 30 seconds
Time interval: 30 seconds
Shear start frame no: 900 (default)
Shear stop frame no: 1800 (default)

Step 2:

Run VI
Select type of flow expt: Pre-During-Post (default)
Select analysis directory: folder which contains vesicle 0, 1, 2.. folders

Step 3:

The program automatically calculates XY centroid (nm), XY centroid (pixel), MSD vs Tau for different conditions
Stops automatically.

Also, XY all vesicles.xls contains XY centroid (nm) of all vesicles. This helps to compare trajectories of all vesicles.

Step 4:

Run the 'READ all MSD vs Tau txt file' VI
This program generates a single MSD vs T ALL txt file. Convert to xl sheet to compare all MSDs.

EXCEL ANALYSIS (FORMULAS) http://en.wikipedia.org/wiki/Equipartition_theorem
STEP 1: Copy all xy centroid (nm) values into 2 columns (assume A and B)

STEP 2: Make new columns (Assuming D and E) with formula " $=A2-A1$ ", click and drag formula for all values. This finds the difference between each reading

STEP 3: Type in formula " $=SQRT(SUMSQ(D:D)/COUNT(D:D))$ ", this solves for the root mean squared (RMS) of all the specified values in the D column

Step 4: Use the Boltzman constant (k_b) = $1.38e-23$ J/K and find temperature value in Kelvin $T = 298$ (room temp), plug and play values into this formula: spring constant (k) = $(k_b * T) / (x^2) * 1e24$ in pN/um

Academic Vita

David J Bernick

484-767-0182 • dbernick@psu.edu

Current Address:

619 W. College Ave Apt. 1
State College, PA 16801

Permanent Address:

1796 Valley Road
Northampton, PA 18067

Objective

To obtain a full time position in a Research & Development career.

Education

Bachelor of Science in Bioengineering; Mechanical Engineering Option
The Pennsylvania State University, University Park, PA Expected May 2012

Schreyer Honors College

- Minors: Engineering Mechanics; Engineering Leadership and Development

Relevant Courses

- Design of mechanical components and structures with anatomical similarities and applications
- Fluid flow systems and properties from pipes to the circulatory system

Biomechanical Technology Lab
Tissue Engineering

Finite Elemental Analysis
Artificial Organs

Related Experiences

Mashavu Project, Khanjan Meta Aug. 2010 – June 2011

Development and implementation of a sustainable telecommunications healthcare system in Kenya.

- Team research, design, and development of instrumentation; measuring the signals of biological systems
- Connected city doctors to distant communities using developed rugged, low cost medical devices

Laboratory Technician, *Dr. Peter Butler* Sept. 2009 – Present
The Mechanobiology Lab studies the forces in vascular epithelium and its role in health and disease

- Designed lens and component configuration necessary for updating an optical trap (laser tweezers)
- Calibrated and operated trap for experiments to measure movement and forces of binding reactions

Teaching Assistant, Dr. Schumann

2012 Spring Semester

- Provided guidance and leadership for class teams to bring their designs from idea to a final prototype

International Engineering Envoy, *Global Engineering Education*

2011–12 academic year

- Held daily office hours and presentations to promote international opportunities for engineering students

Subway Restaurants, State College, PA

Dec. 2008 - Present

- Providing excellent customer service, working about 20 hours per week, preparing food and closing

Activities

Biomedical Engineering Society - Fall 2009 to Present

- Mentor – volunteer position paired up with an underclassman to provide guidance
- Blood Drive Chair - Organized blood drive events, recruited volunteers, and encouraged blood donations

Multicultural Engineering Program - Fall 2007 to Present

Honors and Awards

Recipient of the Diefenderfer Scholarship from the College of Engineering - 2011-12 academic year

Eagle Scout - January 5, 2006

- Final project - comprised of repairing, replacing, and sealing the fencing along the 7 mile Nor-Bath Trail

Dean's List at The Pennsylvania State University – Seven semesters

Skills and Certifications

Professional Lean-Sigma™ Process Improvement – Yellow Belt Certificate

Computer – MATLAB, Solidworks, ANSYS, Abaqus, LabView, COMSOL, MS Office